This paper is a non-peer reviewed preprint submitted to *EarthArXiv*. The manuscript was submitted to *Global Change Biology* for peer review. Future updates on this manuscript will be provided once it's peer-reviewed or accepted. Please feel free to contact me at: shiche@oregonstate.edu if you have any questions or feedbacks.

Scaling High-resolution Soil Organic Matter Composition to Improve Predictions of Potential Soil Respiration Across the Continental United States

Cheng Shi[a], Maruti Mudunuru[b], Maggie Bowman[c], Qian Zhao[c], Jason Toyoda[c], Will Kew[c], Yuri Corilo[c], Odeta Qafoku[c], John R. Bargar[c], Satish Karra[c], & Emily Graham[d,e*]

[a]Oregon State University, Department of Biological & Ecological Engineering, Corvallis, OR, United States.
[b]Energy and Environment Directorate, Pacific Northwest National Laboratory, Richland, WA, United States.
[c] Environmental Molecular Science Laboratory, Pacific Northwest National Laboratory, Richland, WA, United States.
[d]Earth and Biological Sciences Directorate, Pacific Northwest National Laboratory, Richland, WA, United States.
[e]School of Biological Sciences, Washington State University, Pullman, WA, United States.

*Corresponding author: emily.graham@pnnl.gov

Abstract

Despite the importance of microbial respiration of soil organic matter (SOM) in regulating carbon flux between soils and the atmosphere, soil carbon (C) cycling models remain primarily based on climate and soil properties, leading to large uncertainty in their predictions. Molecular data have long been proposed as a promising avenue for resolving modeling errors, but evidence for improved predictions of soil C cycles with high-resolution measurements remains mixed. With data from the 1000 Soils Pilot of the Molecular Observation Network (MONet), we developed a workflow to analyze the molecular composition of water-extractable SOM from 66 soil cores across the United States to address this knowledge gap. Our innovation lies in using machine learning (ML) to distill the thousands of SOM formula that we detected per sample into tractable units; and it enables data from state-of-science measurement techniques to be filtered into the molecules that most directly explain soil respiration. Then, we compared ML predictions of measured potential soil respiration using (1) a suite of standard soil physicochemical data, (2) ultrahigh-resolution SOM composition independently, and (3) in combination with physicochemistry to assess the added value of molecular information to predict soil respiration. In surface soils (0-10 cm), SOM chemistry alone provided better estimates of potential soil respiration than soil physicochemical factors alone, and using the combined sets of predictors yielded the best prediction of soil respiration. In contrast, in subsoils (>10 cm), SOM composition did not improve respiration model performance, possibly due to the importance of mineral-associated SOM below the surface layer. Our workflow is applicable to multiple types of mass spectrometry data and to studies on environmental changes ranging from localized

experiments to global surveys. We underscore the advances of ML tools in downscaling the thousands of SOM molecules detected by state-of-science mass spectrometry for developing new carbon cycling models.

Introduction

Soil respiration is estimated to release 60-100 Gt of C to the atmosphere per year,[1, 2] six to ten times as much C as released by fossil fuel combustion (~10 Gt C[3]). Microbial respiration of soil organic matter (SOM) is one of the most important contributors to soil carbon dioxide (CO_2) emissions and a critical link in the global C cycle.[4] With increasing temperatures under climate change, soil C repositories are vulnerable to increased rates of microbial respiration,[5-7] which can lead to positive feedbacks in global CO_2 emissions and temperature rises.[8] Despite decades of research, soil C fluxes remain one of the largest uncertainties in global climate predictions.[9-14] Novel molecular measurements have recently been applied to identify SOM composition in an effort to understand molecular-scale processes that could improve model predictions of CO_2 fluxes.[15-18] Despite these efforts, our attempts to improve soil C model predictions by refining chemical pools have yielded mixed results.[19-21]

The interplay of factors such as soil moisture, pH, nutrients, mineralogy, and SOM concentration and chemistry governs microbially-derived transformations of SOM;[22-27] but these relationships are difficult to constrain.[4, 28] The most commonly used modeling approaches are based on Raich's model, which estimates respiration primarily as a function of temperature and water availability.[29], [30] Newer process-based model formulations use an additional suite of physical and biogeochemical measurements to represent microbial and mineral processes. They incorporate SOM chemistry either through several discrete pools or through their thermodynamic properties.[21, 31-34] With large spatiotemporal heterogeneity and limited availability of comprehensive and standardized measurements at regional-to-continental scales, accurate predictions of microbial SOM decomposition across different ecosystems remain challenging.[35]

A better understanding of SOM concentration, composition, and bioavailability may enhance our ability to predict soil C cycling processes through their controls on soil respiration and related enzymatic activities.[21, 31-34] Yet, we have little ability to extract meaningful information from the thousands of molecules detected by state-of-science measurements. Variations in the bioavailability of chemical classes of SOM are mediated by geochemical conditions and biophysical constraints, such as microbial biomass and necromass, reactive metals and minerals,

organic and mineral horizon thickness, and other climate-related variables.[36] For example, coarse-textured soil is more conducive to decomposition of chemically labile litter-derived C potentially due to higher fungal activity in organic-rich horizons.[37, 38] In addition, the interface between fresh litter inputs and soil minerals can serve as a hotspot for microbial breakdown of C found in the litter, resulting in the formation of soil aggregates and organo-mineral associations.[39] This variability underlines the essential need to identify unique subsets of SOM formula that contribute more to soil respiration among different ecosystems and soil depths.

Although high mass resolution measurements can provide unprecedented characterization of the thousands of individual formulae that comprise SOM, the interpretation of these data types largely remains guided by coarse chemical and ecological groupings. Unsupervised machine learning models that summarize large data into a small number of significant features have been widely used to study microbial communities, SOM composition, and other environmental problems with multidimensional data.[40] Here, we develop models using semi-supervised machine learning (non-negative matrix factorization with custom *k*-means clustering, NMF*k*) to reduce the complexity of molecular information into *k* distinct signatures of water-extractable SOM chemistry at two depths in cores collected across the continental United States. We then explore the extent to which these signatures and NMF*k*-enabled feature set can provide additional insight into rates of soil respiration beyond variables that are more routinely collected. Our novel workflow results in a 1,000-fold decrease in SOM pool complexity, and the extracted SOM signatures can improve predictions of soil potential respiration ~~a~~across soils from vastly different ecosystems. The enables data from state-of-science measurement techniques to be filtered into the molecules that most directly explain soil respiration. Our workflow is applicable to multiple types of mass spectrometry data and to studies ranging from localized experiments to global surveys.

Methods

Soil sampling and characterization.

As part of the 1000 Soils Pilot study for the Molecular Observation Network (MONet) program, we collected 66 soils from across the continental US using standardized sampling procedures described by Bowman et al.[41] (Figure S1). Two long cores (30 cm) and three short cores (10 cm) were collected at each site. We also conducted field measurements, including soil temperature, volumetric water content, vegetation type, and weather conditions. Cores were shipped on ice overnight to the Pacific Northwest Laboratory for further analysis. A full description of sampling and analytical methodologies is available in Supporting Information and Bowman et al.[41]

Water extractable SOM characterization.

We extracted water-soluble SOM from soils using solid phase extraction and analyzed using a Bruker 7-T Fourier transform ion cyclotron resonance mass spectrometry (FTICR MS) at the Environmental Molecular Sciences Laboratory (EMSL) in Richland, WA. More details on SOM extraction methods and FTICR MS analysis are in Supporting Information and Bowman et al.[41]

Raw FTICR MS data was processed with CoreMS (Python package, installed on 2022/11/22),[42] including signal processing, peak detection, and molecular formula assignment. Noise thresholding was performed with signal-to-noise threshold (5 std.), mass error (0.3 ppm), and stoichiometric limits from domain knowledge (supporting information). Suwannee River fulvic acid (SRFA) standards were used to set a calibration threshold for all soils in the same batch. Molecular formula was assigned based on both accurate mass and filtered by their confidence score from CoreMS. After calibration and formulae assignment, we filtered the assigned peaks by *m/z* between 200 to 1,000, present in at least 2 out of 3 replicates, not present in two or more lab blanks, and with formulae confidence scores (combines *m/z* error and isotopic pattern)[42] above 0.7. We predicted compound classes of the filtered formulae based on O/C

and H/C ratios of van Krevelen classes.[43, 44] The suffix "-like" in chemical classes indicates the uncertainty of the van Krevelen classification method.[44] We converted the peak intensity values to present/absent (1/0) and separated the final dataset by soil depth (surface vs. subsoil) for statistical analysis. Alpha diversity was calculated as the total number of SOM formulae identified in each sample.

Data analysis and machine learning methods.

We used linear regression models to evaluate the relationship between soil potential respiration and soil physicochemical variables. To avoid the impacts of different magnitudes of the data that might lead to biased relationships, we performed $\log_{10}$ transformation on potential respiration rates, total C, total N, total sulfur, and Mn concentration. *stats.linregress* function from *scipy* package (v 1.11.4) in Python (v 3.7.1) was applied to calculate the fitted line, r^2 value ($rvalue^2$, Pearson correlation), and p-value (*pvalue*). Pairwise plots with regression fitting were generated by the pairplot function from the *seaborn* package (v 0.12.1) in Python.

We used non-negative matrix factorization (NMF)[45] with custom k-means clustering (NMF*k*)[46] to identify signature components from the 7312 and 5515 SOM molecular formula (for surface and subsoil, respectively) we detected (i.e., *N* formulae in *m* soils) with *pyNMFk* package (Python, https://github.com/lanl/pyDNMFk, Figure 1). More details on NMF*k* assumptions, model settings, and model robustness are in the Supporting Information. Briefly, NMF*k* tends to be more successful at extracting explainable basis or signatures from large multivariate datasets, compared to other dimensionality reduction tools such as principal component analysis.[45, 47] As applied here, NMF*k* summarizes data into discrete signatures that contain weights for each SOM formulae detected by FTICR-MS for each soil layer independently (i.e., a separate set of signatures was generated to summarize surface versus subsoils, allowing us to explore depth-specific relationships with potential soil respiration). The optimal number of signatures was determined from silhouette coefficients of different NMF*k* models. A W-matrix with the weights of each SOM formulae (*N*) to each extracted signature (*k*), and an H-matrix with the contribution of each signature (*k*) to each soil sample (*m*) were generated from NMF*k*. To visualize the composition of each NMF*k* signatures (W-matrix), we

generated a heatmap of SOM formula with normalized weights (0-1) >0.5 in at least one NMF*k*, clustered by van Krevelen class assignment (clustermap function from seaborn package). Within each inferred chemical class of SOM formula, we further clustered formula using the "linkage" method from the *scipy* package ("ward" method with "Euclidean" distance) to illustrate the difference between NMF*k* signatures.

To define groups of soils with high, medium, or low rates of potential respiration, we used *k*-means clustering on potential soil respiration with the elbow method to select the number of groups (*KMeans* from *scikit-learn* package).[48] Then, we mapped the extracted k signatures to soil respiration using supervised machine learning. To evaluate the potential value of NMF*k*-extracted SOM signatures for explaining soil respiration, we conducted three sets of machine learning models: (1) selected environmental parameters alone (i.e., variables with R^2 >0.2 in individual regressions, Figure 2, Table S1), (2) SOM composition alone (NMF*k* weights from H-matrix), and (3) environmental and SOM composition in combination. All machine learning models were built using gradient boosting regression (GBR) from *scikit-learn* package (v. 0.24, Python). More details in model training, testing and validation are in Supporting Information.

Results

Soil physicochemistry and potential respiration

Overall, many soil parameters, including potential soil respiration, tended to be higher in surface soils than in subsoils. Significant differences ($p<0.05$) between surface soils and subsoils in total C, total N, total sulfur, C/N ratio, and other factors are shown Figure S3. In particular, surface soils had higher potential respiration rates (median: 72.6 ug CO_2/g soil/day) than subsoils (median: 21.9 ug CO_2/g soil/day) (Mann–Whitney U = 3022.5, $N_{surface}$ = 63, $N_{subsoil}$ = 61, P < 0.05).

We grouped potential soil respiration into 3 levels corresponding to low, medium, and high respiration in each soil layer using k-means clustering (Figure S2). For both surface and subsoils, soil with high potential respiration tended to be sourced from the Midwestern and Northeastern United States. (Figure 3, Figure S5). In surface soil, high potential respiration was associated

with five soils collected in Utah, Wyoming, and Virginia (within temperate conifer forest and temperate broadleaf & mixed forest biomes, Figure 3, Figure S1). In subsoils, high respiration was associated with three soils from Utah and Maryland (temperate conifer forests and broadleaf & mixed forests biomes). Desert soils had the lowest respiration in both layers (Figure S1).

We found relationships between soil respiration and many variables that supported prevailing paradigms. A full correlation table of associations between different soil properties is available in the SI (Table S1). Briefly, potential respiration rates in both surface and subsoils were positively correlated with gravimetric water content (GWC) (r^2: 0.246 and 0.225, $p<0.05$) and cation exchange capacity (CEC, r^2: 0.405 and 0.354, $p<0.05$, Figure 2). They were also positively correlated with total C and total N content, with stronger relationships in surface soils (r^2: 0.487 vs. 0.268 for total C, r^2: 0.439 v.s. 0.248 for total N, $p<0.05$). Total bases and magnesium (Mg) concentrations had a higher correlation to respiration in subsoils than surface soils (r^2: 0.227 v.s. 0.146 and 0.287 vs. 0.160, $p<0.05$, Figure 2), while manganese (Mn) concentrations were correlated to respiration in surface soils (r^2: 0.324, $p<0.05$, Figure 2).

SOM composition and NMFk partitioning of SOM.

Across all soils, the most common chemical classes of SOM were lignin-, condensed hydrocarbon-, and tannin-like formula. Most formula in these classes were present in both surface and subsoils (i.e., 'shared' formula). However, surface soils contained more unique formula than subsoils for all compound classes (Figure 3b). In particular, many protein-, amino sugar-, and lipid-like compounds were identified in surface soils only, with very few compounds in these classes being unique to subsoils. Because SOM consists of thousands of different compounds, we also used alpha diversity to represent the SOM richness per sample (Figure 3). Soils from the Midwestern U.S. and the West Coast had relatively higher alpha diversity than soils from other regions.

Then, we used NMF*k* to summarize SOM composition into 7 and 5 NMF*k* signatures, respectively, for surface and subsoils (Figure 4). Geographic patterns in SOM signatures are displayed in Figure S6-7, with more geographic clustering of NMFs in surface soils than in

subsoils. For surface soils, NMF3 presented as the largest relative contributor to SOM composition in 20 soils across all biomes (i.e., highest weighting in H-matrix, hereafter, 'dominant signature', Figure S6). NMF2, NMF5, and NMF7 served as the dominant signature in at least 9 soils each. For subsoils, NMF5 and NMF2 were the dominant signature in 27 soils and 16 soils respectively distributed across all biomes in the continental United States. There was no single NMF signature that could exclusively represent SOM composition of all sites in the same region for either surface or subsoils, suggesting that SOM composition at local sites is best summarized by a combination of multiple NMFs.

The most important formula contributing to the composition of each NMF (i.e., formula with normalized weights >0.5 in W-matrix) are shown in Figure 4a-b. NMF-selected formula (weights >0.5 in W-matrix) generally followed the same general patterns as the overall SOM pool but showed amplified relationships (Figure 4c).

For surface soils, NMF1, 4, 6, and 7 had a relatively high number of important compounds identified as lignin-like. NMF6 and 7 had large contributions of condensed hydrocarbon-like formula. NMF1 had high contribution from protein-like and amino sugar-like compounds, while NMF3 and 5 had the lowest contribution from protein-like, amino sugar-like, and lipid-like compounds of any NMF. NMF4 had the largest number of lipid-like compounds as important features relative to any other surface soil NMF.

In subsoil samples, important formula for all NMFs tended to be classified as lignin-, tannin-, and/or condensed hydrocarbon-like. NMF1 and NMF5 had a larger fraction of features identified as lignin-like compounds than other NMFs in subsoils. NMF2 and NMF3 had a larger fraction of condensed hydrocarbon-like compounds than other NMFs, while NMF4 had large contributions of protein-like and amino sugar-like formula (Figure S8).

We also observed differences in the dominant NMF signatures across high-, medium-, and low-respiration soils, particularly in surface soils (Figure 4d-e). High respiration surface soils were characterized by five NMF signatures (1, 2, 3, 6, and 7), with the largest contribution from NMF6. Low respiration surface soils, in contrast, uniquely contained NMF5, and they did not

have any contribution from NMF6. In subsoils, high respiration soils had high contribution of NMF3 and 4, while low respiration soils were disproportionately associated with NMF5.

Relative importance of physicochemistry and SOM composition in potential soil respiration models

We developed gradient-boosting regression models to predict potential soil respiration with (1) physicochemical variables, (2) SOM composition represented by NMF signatures, and (3) both of them combined. Model performances are summarized in Table 1 and Figure 5.

Selected physicochemical variables (consisting of total C, total N, CEC, moisture, Mn (surface), total base (subsoil), and Mg (subsoil) concentration) had significant independent Pearson's correlation to respiration w/ $p < 0.05$ and $r^2 > 0.2$ (Table S1). Physicochemical variables predicted potential respiration rates in surface and subsoils equally well ($R^2 = 0.44$ and 0.43 respectively for testing data). In surface soils, total C, total N, and cation exchange capacity (CEC) were identified as the top 3 most important predictors, followed by Mn concentration and soil moisture (Figure 4). In subsoils, CEC, total N, and soil moisture were the most important predictor, and total C was the least important predictor (Figure S9).

Using SOM composition (NMF signatures) as predictors, we had better model performance in surface soils than in subsoils (testing $R^2 = 0.54$ vs. 0.08), and SOM composition alone predicted more slightly variation in potential respiration rates than physicochemical variables alone in surface soils (testing $R^2 = 0.54$ vs. 0.44), even when controlling for an equal number of predictors (testing $R^2 = 0.48$ vs. 0.44). NMF3, NMF5, and NMF2 were the most important SOM composition variables for explaining soil respiration in surface soils (Figure 5).

When we combined both physicochemical variables and SOM composition into a single predictor set, we obtained better respiration model performance ($R^2 = 0.62$) compared to models with environmental variables or SOM composition in surface soils only. However, the model describing potential respiration rates in subsoil was worse ($R^2 = 0.36$) when compared to models based on physicochemical variables only. In surface soils, the 3 most important variables were

the same as the physicochemical model (Figure 5). NMF6 was identified as the most important SOM variable, followed by NMF3, NMF2, and NMF5 (Figure 5).

Discussion

Depth partitioning in relationships between SOM composition and potential soil respiration

Given that not all chemical constituents of SOM contribute to soil respiration and that surface and subsoils differ substantially in mineralogy and structure, we hypothesized that distinct subsets of SOM would contribute to respiration in surface vs. subsoils. There was no single NMF that dominated low- vs. high-potential respiration soils in either layer, however, NMF weightings varied substantially across soils with different rates of potential respiration in both layers (Figure 4d-e). This suggests that different subsets of SOM were disproportionately associated with soils exhibiting high vs. low potential respiration rates. While patterns in SOM chemical across geographic regions were difficult to disentangle, the spatial distribution of NMF types suggested local similarity in SOM composition in both layers (Figure S6-7), likely reflecting similar underlying chemistry, mineralogy, and/or biogeochemical processes.[49]

The distillation of multidimensional SOM composition profiles into a tractable set of formula that influence soil respiration is a key challenge in soil ecology.[15, 28, 50-55] The SOM formula within NMFs that correspond to changes in soil respiration may represent a key step forward in understanding the chemical bioavailability of water-extractable organic matter in soils; and our approach can be used with multiple different extraction types and/or high-resolution mass spectrometry measurements. Our results are particularly promising for surface soils, where the dissolved SOM pool (e.g., water-extractable SOM) is thought to fuel microbial respiration. The comparatively weak relationship between subsoil water-extractable SOM and potential soil respiration as compared to surface soils highlights recent work emphasizing the importance of mineral-associated organic matter in soil C storage.[56-58] We therefore suggest that combining our analytical workflow with measurements on mineral-associated organic matter specifically would increase our understanding of SOM cycling in deeper soil layers.

In surface soils, NMF6 displayed a dramatic increase in weighting from low-to-high respiration soils. It contained a diverse suite of compounds including protein-, (soluble) lipid-, and amino sugar-like formula that can be rapidly used as microbial substrate. Proteins and amino sugars in particular can bolster microbial metabolism of SOM,[59, 60] thus the prevalence of these compounds within NMF6 may support high potential rates of soil respiration. NMF1 and NMF7 in surface soils contained a diverse mixture of compounds and also increased from low-to-high respiration soils, supporting a possible relationship between SOM pool diversity and microbial respiration (see previous section). In contrast, surface NMF2, NMF3 and NMF5 decreased in importance from low-to-high respiration soils and primarily consisted of a small but unique subset of lignin- and tannin-like compounds (Figure 4a). This is consistent with low bioavailability of its chemical constituents suppressing microbial respiration.[61, 62] It suggests that despite the often-inferred high bioavailability of water-extractable SOM,[51, 63] there may be a significant fraction of water-extractable SOM that is chemically protected from microbial decomposition.[50, 51, 60] Interestingly, NMF4 in surface soils — which contained the greatest number of lipid-like formula (Figure 4a) and had a comparatively large fraction of protein-like formula —was not present in any high-respiration soils. We therefore suggest that NMF4 may be an indicator of non-living microbial biomass (i.e., necromass) which is disproportionately comprised of lipids (microbial cell wall remnants) and amino sugars and proteins (the basis of intracellular materials).[64, 65]

While these results are broadly consistent with contemporary understanding of the behavior of coarse groups of SOM chemistries, there is substantial variation in SOM bioavailability within most chemical classes of SOM. NMF*k* provides specific subsets of molecules that correspond to soil respiration of at the continental scale. It allows us to downscale from the thousands of molecules detectable by state-of-science methods into more tractable units for further investigation. This is a significant advance, as it allows for more detailed experimentation into and model representation of the precise chemical reactions that leading to the destabilization of SOM. Because the identified molecules are robust across a plethora of different ecosystems, we are hopeful that this workflow can advance generalizable knowledge on soil carbon cycling.

Relative importance of physicochemistry and SOM composition in predicting potential soil respiration

By developing machine learning models to predict respiration with soil physicochemistry and SOM composition (NMFs) separately and in combination, we were able to distinguish the contributions of each set of factors for predicting soil potential respiration. The models based on physicochemistry alone explained a modest amount of variation in soil respiration (44% and 43% in surface and subsoils, respectively), in line with the range of explanatory power observed in other works.[66, 67]

For surface soils, models based on SOM composition alone (54% variation explained) and both physiocochemical factors and SOM composition combined (62% variation explained) suggest that SOM composition (1) can predict soil respiration at least as well as commonly measured physiocochemical variables and (2) explains some portion of soil respiration that is not captured by physiocochemistry. While physicochemical predictors were stronger predictors of soil respiration than SOM composition in the combined surface soil models, the inclusion of SOM composition improved physicochemistry-only models by 18%, indicating that it may significantly impact our ability to predict the rate of soil C cycling processes. NMF3 (which was mainly in low-respiration soil and was comprised of lignin- and tannin-like formula, see previous sections) in particular was the strongest predictor of soil respiration in models based on SOM composition alone followed by NMF2 and NMF5. The relative chemical recalcitrance of the most important predictors of respiration may suggest that the proportion of thermodynamically unfavorable formula in water-extractable SOM has a direct inhibitory effect on soil metabolism. Indeed, thermodynamic regulation of organic C composition can be a key control for the rate of respiration in ecosystems.[50, 51] Therefore, the inclusion of SOM composition in more mechanistic modeling approaches may be able to improve predictions of soil respiration rates.

However, models for subsoils displayed different dynamics. In the subsoil model based on physicochemical variables alone, total C was the least important predictor (vs. the most important predictor for surface soils), and the model containing SOM composition did not yield high predictive power. The marginal effect in partial dependence of surface soil respiration to

total C was stronger than the effect of subsoil respiration (Figure S10), supporting a stronger association between total C and potential respiration in surface soil vs. subsoil. The low predictive power of total C relative to other physicochemical factors could explain why SOM composition did not add predictive power to potential respiration in subsoils. Since more total and organic C is stored in surface soils, resolution into the water-extractable SOM pool (reflected here by NMFs) might be a more significant factor for predicting surface soil respiration than in subsoils that are characterized by lower total C and more mineral-associated SOM.[68]

Our results suggest that NMF-extracted signatures of SOM composition are able to improve surface soil model performance by integrating fundamental molecular information into soil respiration models across very different soil ecosystems at the continental scale. NMF6, which was the most important NMF signature in combined models of surface respiration, consisted of diverse chemically-bioavailable compounds, and it mainly existed in high-respiration soils (see previous sections).[62] We therefore suggest that chemically-bioavailable compounds in water-extractable SOM pools may provide the greatest complementary explanatory power to physicochemical factors in respiration predictions. Because SOM pools vary tremendously at the continental-scale, refined regional or local studies that encompass lower-variability parameter spaces may yield even more value of SOM molecular data to soil C modeling.

Conclusion

Leveraging molecular information of SOM chemistry to improve conceptualizations and models of soil C cycling is a pressing challenge for global biogeochemical and climate predictions. In this study, we develop a machine learning (NMF*k*) workflow to distill the thousands of SOM molecules detected by high resolution mass spectrometry into tractable units that are associated with microbial respiration. By evaluating soil cores collected across the continental United States, we show that these signatures of SOM composition represent subsets of SOM formula which differentially contribute to soils exhibiting low versus high rates of potential respiration. We then disentangle the SOM formula from each NMF*k*-extracted signature and validate their chemical properties in the context of contemporary understandings of SOM bioavailabilty.

Further, subsets of SOM identified by our workflow explained a greater proportion of potential soil respiration than commonly measured physicochemical factors, and they provided additional explanatory power beyond these factors in combined models. Our results provide a new workflow for downscaling the thousands of SOM molecules detected by state-of-science mass spectrometry to spur the development of new process-based modeling of soil C cycles and underscore the advances of NMF*k* in distilling the chemical constituents of SOM that most directly explain soil ecosystem changes.

References

1. Giardina, C.P., et al., *Warming-related increases in soil CO2 efflux are explained by increased below-ground carbon flux.* Nature Climate Change, 2014. **4**(9): p. 822-827.
2. Jian, J., et al., *A restructured and updated global soil respiration database (SRDB-V5).* Earth Syst. Sci. Data, 2021. **13**(2): p. 255-267.
3. Friedlingstein, P., et al., *Global Carbon Budget 2022.* Earth Syst. Sci. Data, 2022. **14**(11): p. 4811-4900.
4. Graham, E.B. and K.S. Hofmockel, *Ecological stoichiometry as a foundation for omics-enabled biogeochemical models of soil organic matter decomposition.* Biogeochemistry, 2022. **157**(1): p. 31-50.
5. Lei, J., et al., *Temporal changes in global soil respiration since 1987.* Nature communications, 2021. **12**(1): p. 403.
6. Nissan, A., et al., *Global warming accelerates soil heterotrophic respiration.* Nature Communications, 2023. **14**(1): p. 3452.
7. Melillo, J.M., et al., *Long-term pattern and magnitude of soil carbon feedback to the climate system in a warming world.* Science, 2017. **358**(6359): p. 101-105.
8. Bond-Lamberty, B. and A. Thomson, *Temperature-associated increases in the global soil respiration record.* Nature, 2010. **464**(7288): p. 579-582.
9. Todd-Brown, K.E., et al., *Causes of variation in soil carbon simulations from CMIP5 Earth system models and comparison with observations.* Biogeosciences, 2013. **10**(3): p. 1717-1736.
10. Todd-Brown, K., et al., *Changes in soil organic carbon storage predicted by Earth system models during the 21st century.* Biogeosciences, 2014. **11**(8): p. 2341-2356.
11. Bradford, M.A., et al., *Managing uncertainty in soil carbon feedbacks to climate change.* Nature Climate Change, 2016. **6**(8): p. 751-758.
12. Davidson, E.A. and I.A. Janssens, *Temperature sensitivity of soil carbon decomposition and feedbacks to climate change.* Nature, 2006. **440**(7081): p. 165-173.
13. Warner, D., et al., *Spatial predictions and associated uncertainty of annual soil respiration at the global scale.* Global Biogeochemical Cycles, 2019. **33**(12): p. 1733-1745.
14. Crowther, T.W., et al., *Quantifying global soil carbon losses in response to warming.* Nature, 2016. **540**(7631): p. 104-108.
15. Billings, S.A., et al., *Soil organic carbon is not just for soil scientists: measurement recommendations for diverse practitioners.* Ecological Applications, 2021. **31**(3): p. e02290.
16. Liang, C., et al., *Quantitative assessment of microbial necromass contribution to soil organic matter.* Global change biology, 2019. **25**(11): p. 3578-3590.
17. Sanderman, J., et al., *Soil organic carbon fractions in the Great Plains of the United States: an application of mid-infrared spectroscopy.* Biogeochemistry, 2021. **156**(1): p. 97-114.
18. Bahureksa, W., et al., *Soil organic matter characterization by Fourier transform ion cyclotron resonance mass spectrometry (FTICR MS): A critical review of sample preparation, analysis, and data interpretation.* Environmental science & technology, 2021. **55**(14): p. 9637-9656.
19. Cotrufo, M.F., et al., *The M icrobial E fficiency-M atrix S tabilization (MEMS) framework integrates plant litter decomposition with soil organic matter stabilization: Do labile plant inputs form stable soil organic matter?* Global change biology, 2013. **19**(4): p. 988-995.
20. Sulman, B.N., et al., *Microbe-driven turnover offsets mineral-mediated storage of soil carbon under elevated CO2.* Nature Climate Change, 2014. **4**(12): p. 1099-1102.
21. Robertson, A.D., et al., *Unifying soil organic matter formation and persistence frameworks: the MEMS model.* Biogeosciences, 2019. **16**(6): p. 1225-1248.
22. Falloon, P., et al., *Direct soil moisture controls of future global soil carbon changes: An important source of uncertainty.* Global Biogeochemical Cycles, 2011. **25**(3).
23. Ciais, P., et al., *Carbon and other biogeochemical cycles*, in *Climate change 2013: the physical science basis. Contribution of Working Group I to the Fifth Assessment Report of the Intergovernmental Panel on Climate Change*. 2014, Cambridge University Press. p. 465-570.
24. Amador, J. and R.D. Jones, *Nutrient limitations on microbial respiration in peat soils with different total phosphorus content.* Soil Biology and Biochemistry, 1993. **25**(6): p. 793-801.
25. Malik, A.A., et al., *Land use driven change in soil pH affects microbial carbon cycling processes.* Nature communications, 2018. **9**(1): p. 3591.
26. Fang, C. and J.B. Moncrieff, *The variation of soil microbial respiration with depth in relation to soil carbon composition.* Plant and Soil, 2005. **268**: p. 243-253.

27. Curiel Yuste, J., et al., *Microbial soil respiration and its dependency on carbon inputs, soil temperature and moisture.* Global Change Biology, 2007. **13**(9): p. 2018-2035.
28. Billings, S.A. and F. Ballantyne IV, *How interactions between microbial resource demands, soil organic matter stoichiometry, and substrate reactivity determine the direction and magnitude of soil respiratory responses to warming.* Global Change Biology, 2013. **19**(1): p. 90-102.
29. Raich, J.W. and C.S. Potter, *Global patterns of carbon dioxide emissions from soils.* Global biogeochemical cycles, 1995. **9**(1): p. 23-36.
30. Raich, J.W., C.S. Potter, and D. Bhagawati, *Interannual variability in global soil respiration, 1980–94.* Global Change Biology, 2002. **8**(8): p. 800-812.
31. Kyker-Snowman, E., et al., *Stoichiometrically coupled carbon and nitrogen cycling in the MIcrobial-MIneral Carbon Stabilization model version 1.0 (MIMICS-CN v1. 0).* Geoscientific Model Development, 2020. **13**(9): p. 4413-4434.
32. Wieder, W.R., et al., *Carbon cycle confidence and uncertainty: Exploring variation among soil biogeochemical models.* Global change biology, 2018. **24**(4): p. 1563-1579.
33. Waring, B.G., et al., *From pools to flow: The PROMISE framework for new insights on soil carbon cycling in a changing world.* Global Change Biology, 2020. **26**(12): p. 6631-6643.
34. Song, H.-S., et al., *Representing organic matter thermodynamics in biogeochemical reactions via substrate-explicit modeling.* Frontiers in Microbiology, 2020. **11**: p. 531756.
35. Bradford, M.A., et al., *Quantifying microbial control of soil organic matter dynamics at macrosystem scales.* Biogeochemistry, 2021. **156**(1): p. 19-40.
36. Hall, S.J., et al., *Molecular trade-offs in soil organic carbon composition at continental scale.* Nature Geoscience, 2020. **13**(10): p. 687-692.
37. Huys, R., et al., *Plant litter chemistry controls coarse-textured soil carbon dynamics.* Journal of Ecology, 2022. **110**(12): p. 2911-2928.
38. Scott, N.A., et al., *Soil textural control on decomposition and soil organic matter dynamics.* Soil Science Society of America Journal, 1996. **60**(4): p. 1102-1109.
39. Witzgall, K., et al., *Particulate organic matter as a functional soil component for persistent soil organic carbon.* Nature Communications, 2021. **12**(1): p. 4115.
40. Sonnewald, M., et al., *Elucidating ecological complexity: Unsupervised learning determines global marine eco-provinces.* Science Advances, 2020. **6**(22): p. eaay4740.
41. Bowman, M.M., et al., *One thousand soils for molecular understanding of belowground carbon cycling.* Frontiers in Soil Science, 2023. **3**.
42. Corilo, Y., W. Kew, and L. McCue, *EMSL-Computing/CoreMS: CoreMS 1.0. 0 (v1. 0.0).* Zenodo10, 2021. **5281**.
43. Kim, S., R.W. Kramer, and P.G. Hatcher, *Graphical method for analysis of ultrahigh-resolution broadband mass spectra of natural organic matter, the van Krevelen diagram.* Analytical chemistry, 2003. **75**(20): p. 5336-5344.
44. Tfaily, M.M., et al., *Advanced solvent based methods for molecular characterization of soil organic matter by high-resolution mass spectrometry.* Analytical chemistry, 2015. **87**(10): p. 5206-5215.
45. Lee, D. and H.S. Seung, *Algorithms for non-negative matrix factorization.* Advances in neural information processing systems, 2000. **13**.
46. Bhattarai, M., et al. *Distributed Non-Negative Tensor Train Decomposition*. in *2020 IEEE High Performance Extreme Computing Conference (HPEC)*. 2020.
47. Devarajan, K., *Nonnegative Matrix Factorization: An Analytical and Interpretive Tool in Computational Biology.* PLOS Computational Biology, 2008. **4**(7): p. e1000029.
48. Bholowalia, P. and A. Kumar, *EBK-means: A clustering technique based on elbow method and k-means in WSN.* International Journal of Computer Applications, 2014. **105**(9).
49. Brye, K.R., et al., *Environmental controls on soil respiration across a southern US climate gradient: a meta-analysis.* Geoderma Regional, 2016. **7**(2): p. 110-119.
50. Tureţcaia, A.B., et al., *Rethinking Aerobic Respiration in the Hyporheic Zone under Variation in Carbon and Nitrogen Stoichiometry.* Environmental Science & Technology, 2023. **57**(41): p. 15499-15510.
51. Garayburu-Caruso, V.A., et al., *Carbon limitation leads to thermodynamic regulation of aerobic metabolism.* Environmental Science & Technology Letters, 2020. **7**(7): p. 517-524.
52. Hodgkins, S.B., et al., *Changes in peat chemistry associated with permafrost thaw increase greenhouse gas production.* Proceedings of the National Academy of Sciences, 2014. **111**(16): p. 5819-5824.

53. Li, H., et al., *Simple plant and microbial exudates destabilize mineral-associated organic matter via multiple pathways.* Environmental science & technology, 2021. **55**(5): p. 3389-3398.
54. Graham, E.B., et al., *Multi'omics comparison reveals metabolome biochemistry, not microbiome composition or gene expression, corresponds to elevated biogeochemical function in the hyporheic zone.* Science of the total environment, 2018. **642**: p. 742-753.
55. Graham, E.B., et al., *Carbon inputs from riparian vegetation limit oxidation of physically bound organic carbon via biochemical and thermodynamic processes.* Journal of Geophysical Research: Biogeosciences, 2017. **122**(12): p. 3188-3205.
56. Cotrufo, M.F., et al., *Soil carbon storage informed by particulate and mineral-associated organic matter.* Nature Geoscience, 2019. **12**(12): p. 989-994.
57. Benbi, D., A. Boparai, and K. Brar, *Decomposition of particulate organic matter is more sensitive to temperature than the mineral associated organic matter.* Soil Biology and Biochemistry, 2014. **70**: p. 183-192.
58. Lugato, E., et al., *Different climate sensitivity of particulate and mineral-associated soil organic matter.* Nature Geoscience, 2021. **14**(5): p. 295-300.
59. Campbell, T.P., et al., *Microbial Communities Influence Soil Dissolved Organic Carbon Concentration by Altering Metabolite Composition.* Frontiers in Microbiology, 2022. **12**.
60. Hernández, D.L. and S.E. Hobbie, *The effects of substrate composition, quantity, and diversity on microbial activity.* Plant and Soil, 2010. **335**(1): p. 397-411.
61. Kögel-Knabner, I., *The macromolecular organic composition of plant and microbial residues as inputs to soil organic matter.* Soil Biology and Biochemistry, 2002. **34**(2): p. 139-162.
62. Marschner, B. and K. Kalbitz, *Controls of bioavailability and biodegradability of dissolved organic matter in soils.* Geoderma, 2003. **113**(3-4): p. 211-235.
63. Marschner, B. and K. Kalbitz, *Controls of bioavailability and biodegradability of dissolved organic matter in soils.* Geoderma, 2003. **113**(3): p. 211-235.
64. Camenzind, T., et al., *Formation of necromass-derived soil organic carbon determined by microbial death pathways.* Nature Geoscience, 2023. **16**(2): p. 115-122.
65. Angst, G., et al., *Plant- or microbial-derived? A review on the molecular composition of stabilized soil organic matter.* Soil Biology and Biochemistry, 2021. **156**: p. 108189.
66. Graham, E.B., et al., *Do we need to understand microbial communities to predict ecosystem function? A comparison of statistical models of nitrogen cycling processes.* Soil Biology and Biochemistry, 2014. **68**: p. 279-282.
67. Allison, S., *A trait-based approach for modelling microbial litter decomposition.* Ecology letters, 2012. **15**(9): p. 1058-1070.
68. Rumpel, C. and I. Kögel-Knabner, *Deep soil organic matter—a key but poorly understood component of terrestrial C cycle.* Plant and soil, 2011. **338**: p. 143-158.

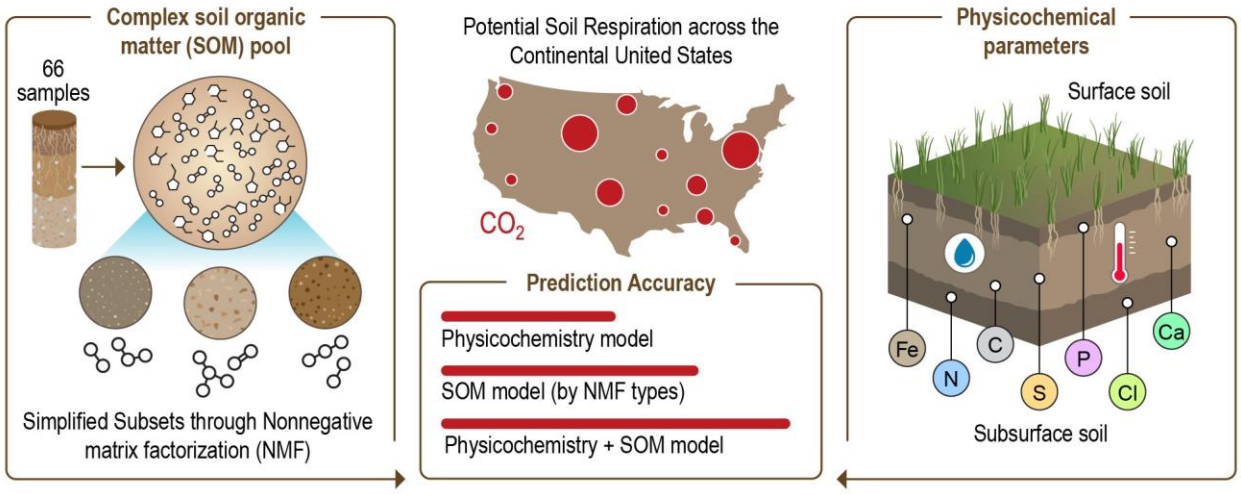

Figure 1. Proposed workflow: Machine learning models summarize molecular data to predict soil respiration. Non-negative matrix factorization (NMF*k*) extracts key SOM signatures from high resolution mass spectrometry measurements of SOM. Gradient boosting regression predicts soil respiration with physicochemistry, SOM signatures, and physicochemistry combined with SOM signatures.

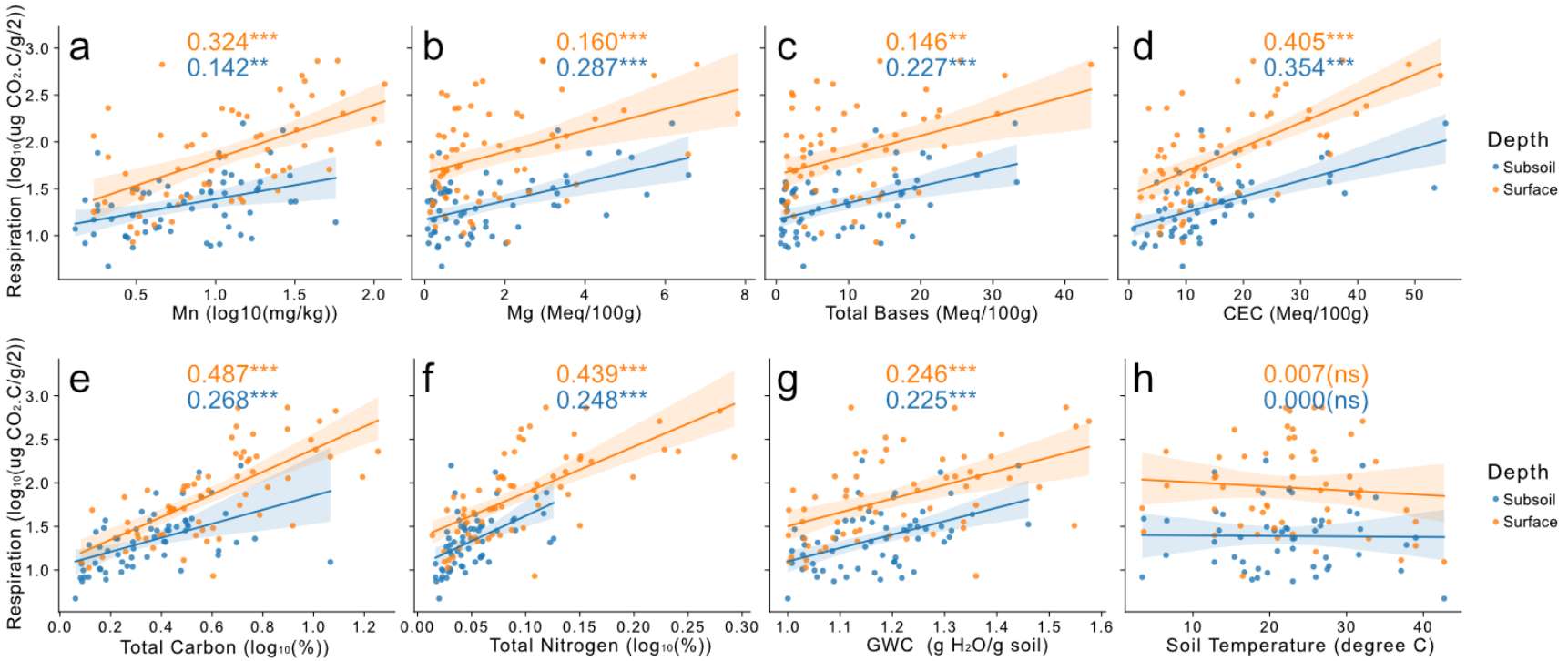

Figure 2. The relationship between soil characteristics and potential respiration. (a-h) show [Manganese(Mn), Magnesium(Mg), Total Bases, CEC, Total C, Total N, GWC, Soil Temperature], respectively. Orange represents surface soils and blue represents subsoils. Lines denote the fitted linear regression function. Numbers on each panel are r^2 value from linear regression, the stars behind represents statistical significance (*** ($p \leq 0.001$), **($p \leq 0.01$), ns ($p > 0.05$)).

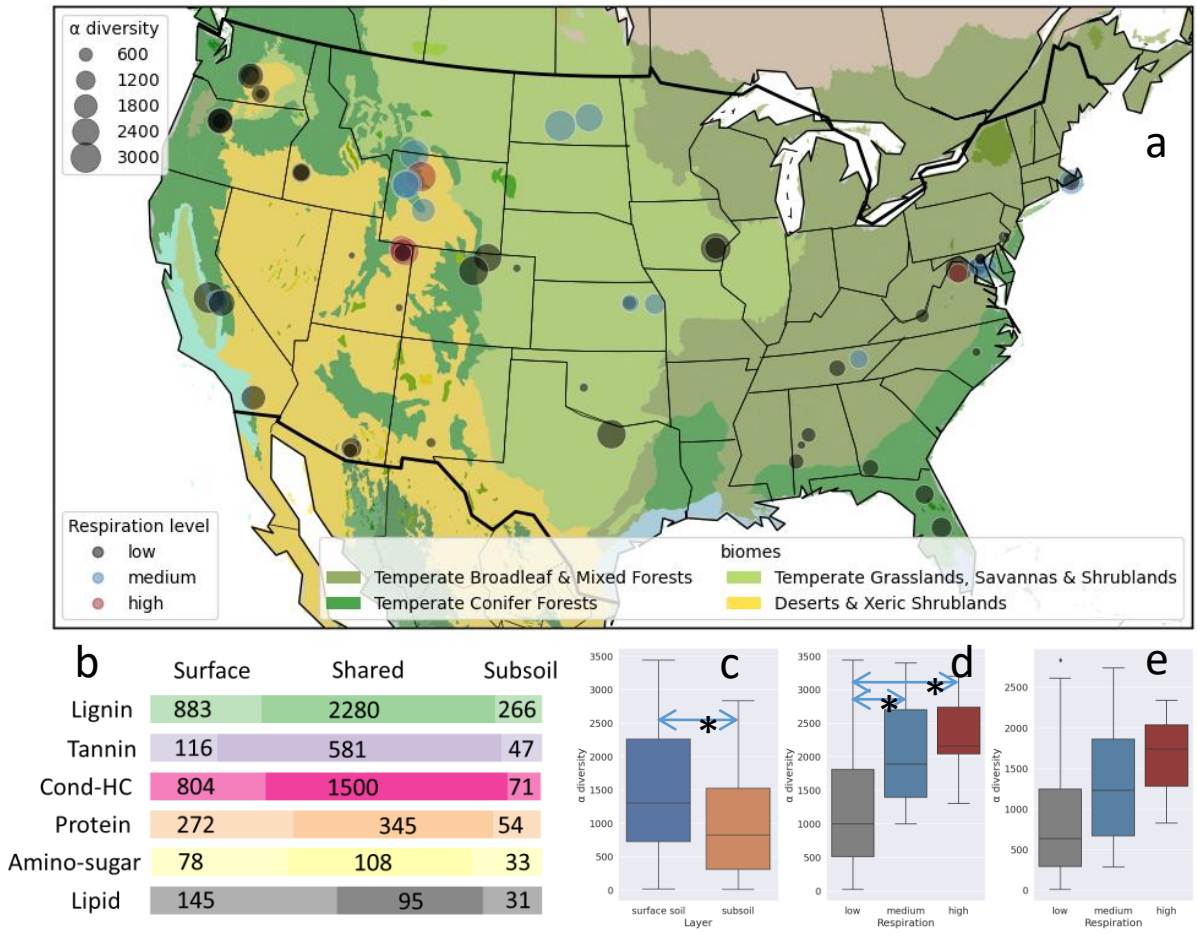

Figure 3. (a) Spatial distribution of soil respiration levels (labeled by colors) and alpha diversity of each sample (sizes). Soil respiration levels are determined by *k*-means clustering on soil respiration rates (ug CO2/g soil/day). Soils from temperate conifer forests and temperate grasslands, savannas & shrublands have relatively higher respiration rates compared to other biomes (Figure S1). (b) The number of shared and unique SOM compound classes identified between surface and subsoils. The classes were suggested by van-Krevelen plot. (c) The difference of alpha diversity in surface and subsoil soils ($p < 0.05$ from ANOVA, *: $p<0.05$ from Tukey's HSD test) (d) the difference of alpha diversity in surface soils with different levels of potential respiration ($p < 0.05$ from ANOVA, *: $p<0.05$ from Tukey's HSD test) (e) the difference of alpha diversity in subsoils with different levels of potential respiration ($p < 0.05$ from ANOVA).

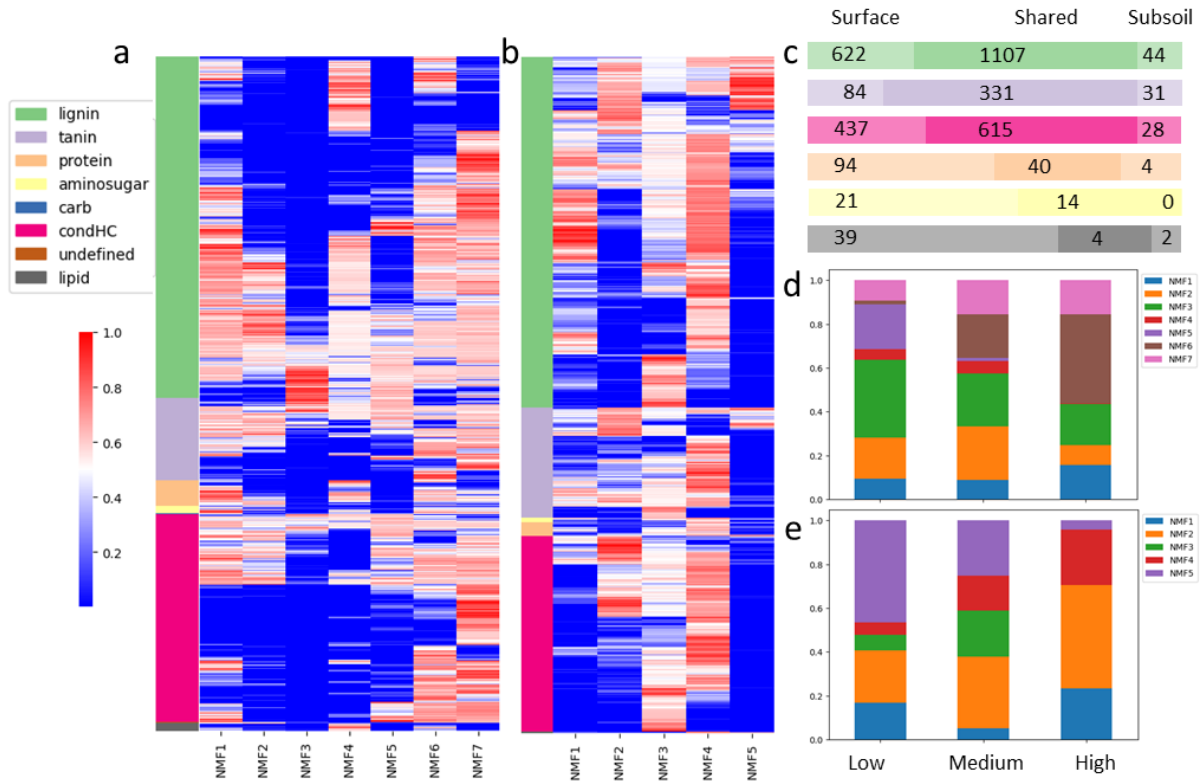

Figure 4. NMF*k* partitioning of SOM composition. (a-b) Relative contribution of organic formula to each SOM signatures identified by NMF*k* in a) surface and b) subsoils. The color in each cell represents the normalized (0 to 1) relative contribution for each SOM feature (row) to each NMF*k* signature (column), red indicates the most important contributor, and blue indicates the least. The side bar indicates the compound class of each SOM feature. (c) The number of shared and unique formula identified as important (normalized weights >0.5) by NMF*k* in surface and subsoils. (d-e) The relative contribution of NMF*k* signatures to each level of respiration rates in both d) surface and e) subsoils. Surface soils: low respiration (N = 44), medium respiration (N = 14), high respiration (N = 5). Subsoils: low respiration (N = 48), medium respiration (N =10), high respiration (N = 3).

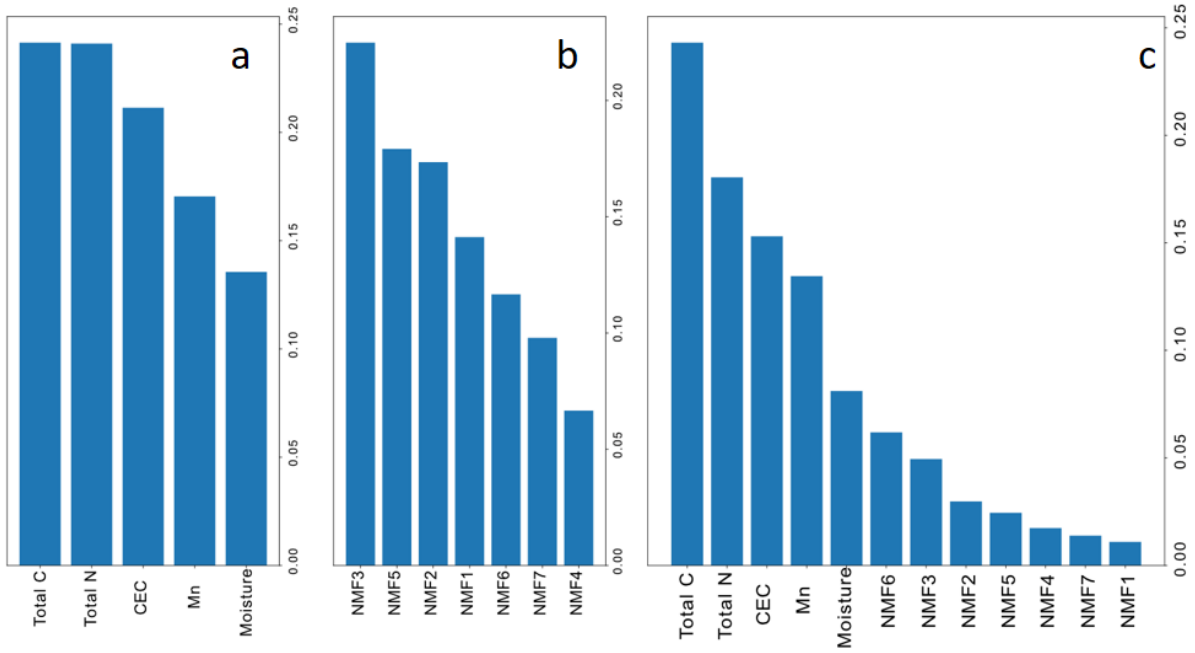

Figure 5. Relative importance of each predictor in surface soil potential respiration machine learning models. a) Physicochemistry model, with physicochemical variables only. b) SOM model, with SOM signatures represented by NMFs only. c) Physicochemistry & SOM model with both physicochemical variables and SOM signatures.

Table 1. Model performance for predictions of potential soil respiration with physicochemical variables (Physiochemistry model), SOM by NMF*k* signatures (SOM_model), and combined physicochemical variables and SOM variables (Physiochemistry &SOM_model) for average 5-fold cross-validation accuracies (training soils, RMSE), and testing sample accuracies (RMSE, R2).

	Physiochemistry Model	SOM_model	Physicochemistry &SOM_model
Surface_CV (RMSE)	0.80	1.05	0.82
Surface_test (RMSE)	0.98	0.89	0.82
Surface_test (R^2)	0.44	0.54	0.62
Subsoil_CV (RMSE)	0.60	0.82	0.67
Subsoil_test (RMSE)	0.46	0.80	0.49
Subsoil_test (R^2)	0.43	0.08	0.36

Supporting Information of

Scaling High-resolution Soil Organic Matter Composition to Improve Predictions of Potential Soil Respiration Across the Continental United States

Cheng Shi[a], Maruti Mudunuru[b], Maggie Bowman[c], Qian Zhao[c], Jason Toyoda[c], Will Kew[c], Yuri Corilo[c], Odeta Qafoku[c], John R. Bargar[c], Satish Karra[c], & Emily Graham[d,e*]

[a]Oregon State University, Department of Biological & Ecological Engineering, Corvallis, OR, United States.
[b]Energy and Environment Directorate, Pacific Northwest National Laboratory, Richland, WA, United States.
[c] Environmental Molecular Science Laboratory, Pacific Northwest National Laboratory, Richland, WA, United States.
[d]Earth and Biological Sciences Directorate, *Pacific Northwest National Laboratory, Richland, WA, United States.*
[e]*School of Biological Sciences, Washington State University, Pullman, WA, United States.*

**Corresponding author: emily.graham@pnnl.gov*

Soil Physicochemistry and SOM composition Analysis

Briefly, once soil cores were delivered to the lab, we divided the 30-cm cores into 10 cm depth intervals, where only the top (hereafter, surface or surficial soil) and bottom (hereafter, subsoil) sections were used for further analysis. We mixed the top sections with three short cores to homogenize the local variation. The soils were then sieved through 4 mm sieves separately to remove rocks and root structures. We measured gravimetric water content (GWC) by drying 10 g of soil for 24 hours in a drying oven at 100 ºC. We measured soil pH by mixing 20 g of dry soil with 20 mL of DI water (1000 rpm on reciprocating shaker for 15 minutes), and tested with a calibrated pH probe. Soil microbial biomass C and nitrogen (N) content were measured via chloroform fumigation.[1-3] We extracted phosphorus contents using Bray ($pH < 7$) or Olsen extractions ($pH > 7$),[4, 5] and extracted nitrate and ammonium with 0.5M K_2SO_4 and tested by colorimetric methods. Ion concentrations of potassium (K), calcium (Ca), magnesium (Mg), and sodium (Na) from 1:10 ammonium acetate extraction, Zinc (Zn), manganese (Mn), copper (Cu), iron (Fe), boron (B), and sulfate (SO_4^{2-}) from 1:2 soil to diethylenetriaminepentaacetic acid (DPTA) extraction were measured using Inductively coupled plasma mass spectrometry (ICP-MS). We measured total C and N using the AOAC official methods 972.43.[6] Soil texture was measured by hydrometer analysis. Finally, we assessed potential soil respiration using the CO_2 burst method with 24 hours of incubation at 24 ºC.[7]

We extracted water-soluable SOM by mixing 6 g of dry soil with 30 ml DI water in triplicates, shaken for 2 hours at 800 rpm, and centrifuged at 6,000 rpm for 8 minutes. 5 ml of supernatant was acidified with 2 µl concentrated phosphoric acid (37%), and then loaded onto Agilent Bond Elut PPL solid phase extraction cartridges[8] with Gilson ASPEC® SPE system. A Bruker 7-T Fourier transform ion cyclotron resonance mass spectrometry (FTICR MS) at the Environmental Molecular Sciences Laboratory (EMSL) in Richland, WA, was used to analyze SOM composition, with a negative ionization mode and ion accumulation time at 0.01 or 0.025 seconds (depending on dissolved organic C concentration). The measured mass accuracy was typically within 1 ppm. One lab blank and one Suwannee River Fulvic Acid (SRFA) sample (20 ppm) were tested every 30 soils to evaluate instrument performance.

NMFk model assumption and robustness

NMF*k* model was selected to decompose the SOM composition matrix into multiple basis signatures, due to its ability to capture unique and sparse characteristics or data patterns [9]. The underlying assumption of NMF*k* is

that there are similar distributions of variables across samples such that the main characteristics of each sample can be represented by the combination of a limited number of non-negative additive components (signatures) [10]. It has also been widely used in environmental forensics [11, 12], text mining [13], face recognition [14]. Vesselinov et al. used NMF*k* to identify unknown recharge sources of groundwater driven by various physical and chemical processes [15]. Cai et al. used NMF to extract key features and reveal temporal changes in microbial communities [16]. Instead of linear transformation of the original dataset by correlations like principal components analysis (PCA), NMF*k* uses non-negativity constraints that makes it better suited to identify representative SOM signatures and evaluate their distribution in different samples. Furthermore, the additive fashion of extracted signatures by different weights in NMF*k* fit the intuition of different pools of SOM molecules combined into the mixture of SOM in a certain sample. Therefore, the NMF*k* extracted SOM signatures are more explainable compared to PCA or other ordination techniques.

The number of dominant types (k) was determined by silhouette coefficient with a threshold of 0.5 to test model stability [17, 18]. The last model above the threshold (> 0.5) is selected as the final model. This is because the selected model should have good separation between different non-negative signatures but also a stable solution at the same time.

Gradient Boosting regression models

Gradient boosting is a machine learning algorithm that combines multiple weak models, such as decision trees, into a stronger model iteratively, where each weak model learns from the residual error from the previous model.[19] It is one of the most powerful and effective machine learning models that is widely used in many different areas. Gradient boosting regression is an ensemble model that iteratively learns from the error of previous model. Using ensemble, it is capable to generate predictions from multiple decision tree models and thus provide a more robust prediction. It usually has better performance with smaller dataset, because it tends less overfit the data [20]. Therefore, it is suitable for predicting soil respiration with physicochemistry and SOM types.

Model hyperparameters were tuned first with 5-fold cross validation on 80% of each dataset (*train_test_split* in scikit-learn, with the same *random_state* for models in the same layer) using *RandomizedSearchCV* function from scikit-learn. We then used the best-tuned parameters with 80% of soils to build the finalized model. Root means square error (RMSE) was used to evaluate the error of models. More details on hyperparameter grids can be found in supporting information. All the models were then tested with the other 20% of soils to compare their performance. The most important predictors for the models with the best performance were then determined using MDI importance and/or mean decrease in impurity to infer potential relationships between soil environmental parameters, SOM composition, and potential soil respiration. Partial dependence plots were used to evaluate the response of potential respiration to the selected important features.

We performed feature selection for physicochemical factors by statistical relevance (Table S1), to remove irrelevant features that likely introduce noise and leads to overfitting of the model.[21, 22] Total C, total N, CEC, Mn and soil moisture were selected as predictors for surface soil models. Total C, total N, total base, CEC, Mg and soil moisture were selected for subsoil models. The detailed settings of hyperparameter dictionary for *RandomizedSearchCV* function and the tunned parameter set used for the final model is in Table S2. To avoid the impacts of the increased number of predictors on improved model performance for surface respiration model (physicochemistry model: n = 5, SOM model: n = 7), we developed another version of SOM model without the two least important predictors (NMF7, NMF4). The model performance was still better (testing R^2 = 0.48 vs. 0.44) compared to the physicochemistry model with the same number of predictors (n = 5).

Soil respiration and physicochemistry

Soil moisture, total C, and total N appeared to regulate soil respiration in both surface soil and subsoil, as evidenced by positive correlations of total C, N, and moisture with potential soil respiration (Figure 2). This is consistent with previous work describing relationships between these properties and soil respiration, as well as other factors that we observed to be correlated with respiration including pH and CEC.[23-26] Soil physical properties (e.g, moisture and pore space connectivity) can constrain microbial access to SOM molecules and nutrients isolated in soil pore networks, thereby regulating microbial respiration of SOM.[26-30] Additionally, C and N can limit soil respiration through stoichiometric constraints on biomass production.[31-34]

We also found a suite of correlations between elements and potential soil respiration that may reflect the influence of vegetation across rooting profiles; however, associations between inorganic nutrients (NH^{4+}, NO^{3-}, PO_4^{3-}) and respiration were conspicuously absent ($p>0.05$, Table S1).[35-38] Mg, Mn, Zn, and sulfate were correlated to potential soil respiration and are known to have strong impacts on plant productivity that provides chemically labile C sources for microbial respiration.[39-41] Mn can also influence soil respiration by regulating the activities of Mn peroxidase enzyme, a lignin-degrading enzyme produced by fungi and *Actinobacteria*.[42-46] Because total N corresponded to potential soil respiration, the lack of relationship between respiration and inorganic nutrients may indicate organic nutrients as key drivers of soil respiration. Alternatively, inorganic nutrient limitations that vary tremendously through space and time may not be observable across different ecosystems at the continental scale.[47, 48]

In addition to patterns in soil physicochemistry, e observed geographic patterns in potential soil respiration that contrasted with some previous estimates,[49] including high rates of potential soil respiration in the midwestern and mid-Atlantic regions, and at high elevations (Figure 3). A notable difference between Nissan et al. and the current study is that Nissan et al. report simulated mean annual values of heterotrophic respiration in soils, while the current study reports the measured potential respiration rates of sieved soils collected during the summer months. Because high latitude and high elevation ecosystems can exhibit intense, short-lived peaks of biomass during summertime,[50] soils collected during this period may have relatively extreme rates of potential respiration that are averaged out at the annual scale. Another interpretation for higher potential soil respiration at high elevation is that relative humidity typically increases with elevation and thus can stimulate higher microbial activities and SOM decomposition.[51] In contrast, comparatively low potential soil respiration recorded in the Southeastern United States could also reflect the comparatively low C content of these soils that has been associated with faster turnover rates and high year-round temperatures.[52]

Variation in SOM composition across soil depths

Differences in SOM composition with soil depth and across the continental United States were associated with potential soil respiration, supporting previous studies showing relationships

between SOM composition and soil respiration rates (Figure 3).[53-55] Regardless of depth or geographic location, the diversity of water-extractable SOM compounds appeared to be a common factor in regulating potential soil respiration — soils with higher potential respiration generally had more diverse pools of water-extractable SOM (Figure 3d-e).

Our results were consistent with a paradigm in which chemically bioavailable, plant-derived molecules including proteins and amino sugars are degraded through soil profiles and transformed into microbially-derived byproducts that are stabilized via organo-mineral associations;[56-58] whereas more chemically recalcitrant compounds (e.g., lignins and tannin) are preserved due to their lower thermodynamic bioavailability.[59-61] Coincident decreases in SOM diversity from surface to subsoils were also associated with decreases in potential soil respiration (Figure 3b-c), further supporting a link between SOM pool composition and microbial decomposition.[61, 62] The comparatively diverse SOM pools in surface soils contained more bioavailable compounds than subsoils, including protein-, amino sugar-, and lipid-like compounds.[63, 64] The number of formulae in these chemical classes declined with depth, and formula that were common to both soil layers primarily included chemical classes with low putative bioavailability such as lignin-, tannin-, and condensed hydrocarbon-like compounds.[64]

In subsoils, NMF4 (associated with high-respiration soils) and NMF5 (associated with low-respiration soils) had the largest disparities in weighting across subsoils (Figure 4e). Consistent with observations from surface soils, subsoil NMF4 contained the largest proportion of amino sugar- and protein-like formula compared to other subsoil NMFs, while NMF5 was almost entirely composed of lignin- and tannin-like compounds.[64] The composition of water-extractable SOM in mineral subsoils is an emerging area of research, and it remains unclear how different SOM chemistries contribute to subsoil respiration.[59] Our results suggest some consistencies in the chemical mechanisms of SOM bioavailability across soil horizons. However, one subsoil NMF (NMF2) had unexpectedly large weightings in high respiration subsoils despite low bioavailability typically associated with its chemical constituents.[64, 65] The remaining subsoil NMFs (1 and 3) were present in both low- and high-respiration subsoils. This denotes that factors beyond chemical recalcitrance or beyond the most commonly measured (water-extractable) SOM pool are critical to understanding belowground C cycling.[66, 67]

193 *Supporting Tables*

194 Table S1. Coefficient of Determination between soil respiration and soil biogeochemistry

195 (Pearson's correlation R-square)

	Surface R^2	Surface p-value	Subsoil R^2	Subsoil p-value
Mn	**0.324**	**0.000**	**0.142**	**0.003**
Mg	**0.160**	**0.001**	**0.287**	**0.000**
K	0.004	0.638	0.053	0.071
Na	0.005	0.577	0.026	0.211
B	**0.119**	**0.006**	0.018	0.295
Zn	**0.173**	**0.001**	**0.102**	**0.011**
Fe	**0.089**	**0.017**	0.043	0.106
Cu	**0.092**	**0.016**	**0.133**	**0.004**
Total Base	**0.146**	**0.002**	**0.227**	**0.000**
CEC	**0.405**	**0.000**	**0.354**	**0.000**
Total C	**0.487**	**0.000**	**0.268**	**0.000**
Total N	**0.439**	**0.000**	**0.248**	**0.000**
Total S	**0.080**	**0.028**	0.036	0.160
GWC	**0.246**	**0.000**	**0.225**	**0.000**
Soil T	0.007	0.545	0.000	0.919
pH	**0.116**	**0.004**	0.007	0.513
SO4	**0.172**	**0.001**	0.002	0.759
P	0.001	0.855	0.003	0.695
NH4	0.002	0.761	0.000	0.992
NO3	0.004	0.634	0.004	0.634

Sand%	**0.140**	**0.001**	**0.176**	**0.000**
Silt%	**0.081**	**0.017**	**0.077**	**0.022**
Clay%	**0.157**	**0.001**	**0.182**	**0.000**
Elevation	**0.136**	**0.006**	**0.090**	**0.029**
alpha_div	**0.159**	**0.001**	**0.143**	**0.003**

196
197
198

199 Table S2. Hyperparameter tunning settings and the tunned hyperparameters used in each model.

Hyperparameter name	param_distributions	Physicochemistry Model		SOM Model		Physicochemistry & SOM Model	
		Surface	Subsoil	Surface	subsoil	surface	subsoil
n_estimators	randint(50,5000)	1213	1722	422	636	1392	351
max_depth	randint(2,60)	31	58	14	7	40	16
max_features	randint(1, X.shape[1])	1	6	2	5	3	7
min_samples_split	randint(2, 10)	6	6	4	6	7	9
learning_rate	[0.0001, 0.001, 0.01, 0.1, 1.0]	0.01	0.01	0.1	0.001	0.1	0.1
ccp_alpha	expon(scale=0.1)	0.0009419401	0.0173195734	0.0435524849	0.0017778767	1.86731365e-05	0.0006595532

200

201

Supporting Figures

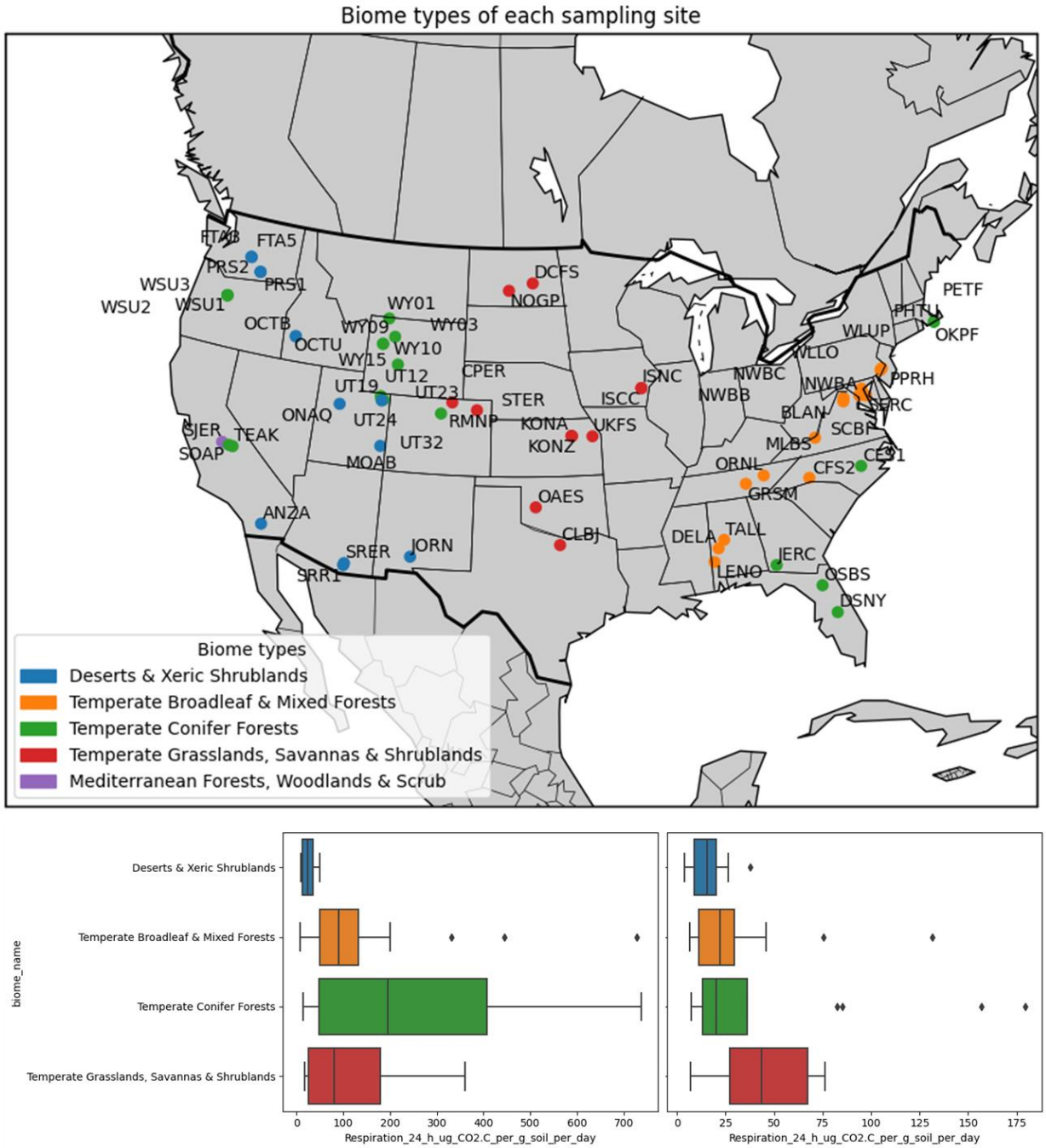

Figure S1. Sampling locations, sample names, and their biome types obtained from WWF terrestrial ecoregions (a). Difference of soil potential respiration by biomes in b) surface and c) subsoil.

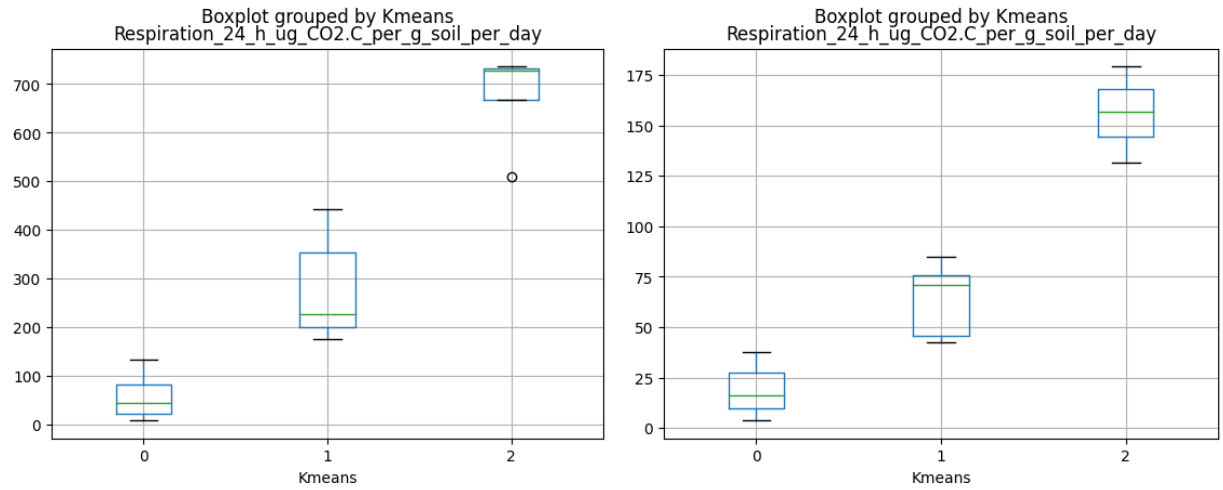

Figure S2. k-means clustering of soil respiration rates at different depths (a: surface soils, b: subsoils). 3 levels of respiration were determined for both surface and subsoil.

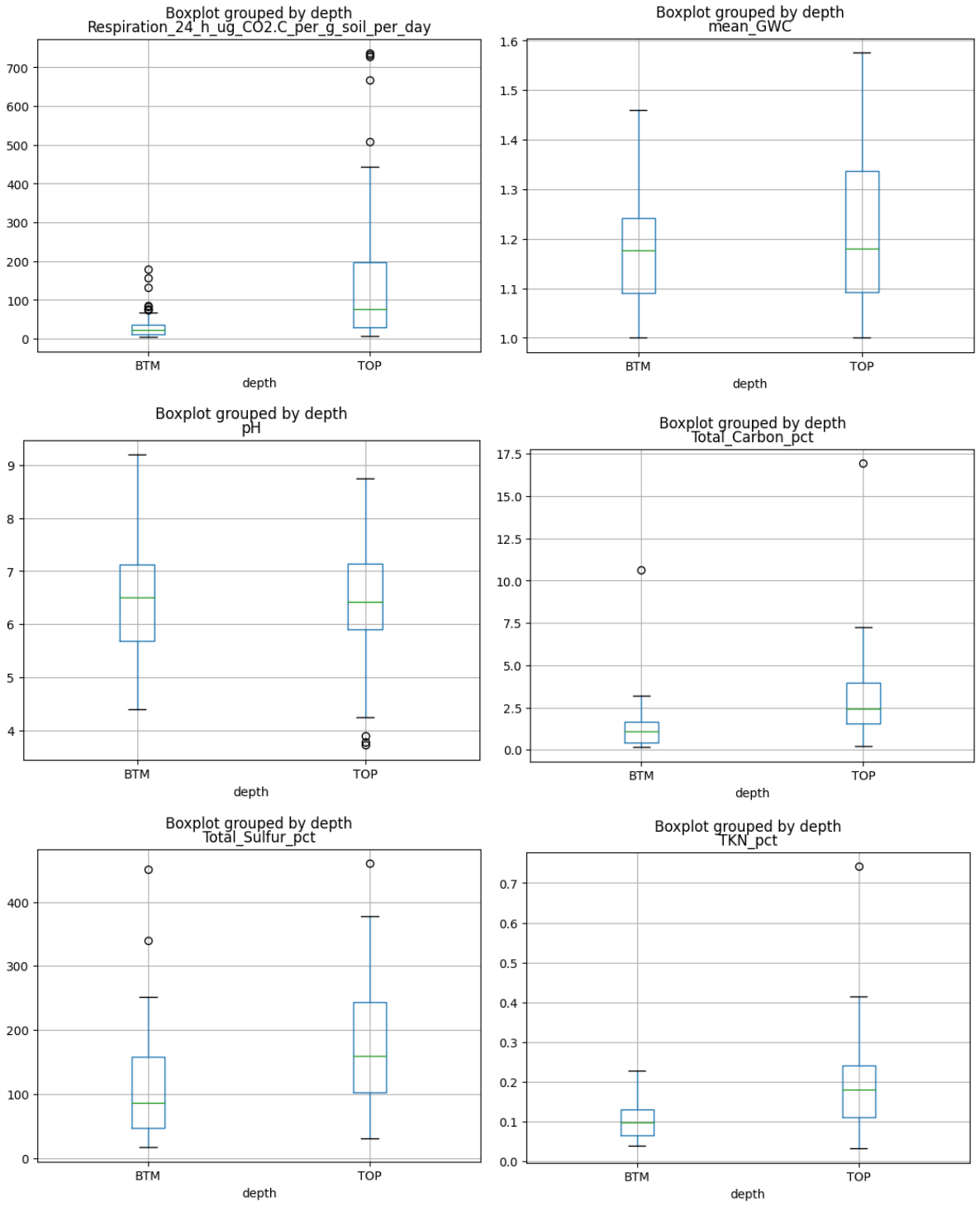

Figure S3. Boxplots of difference in soil biogeochemistry between surface and subsoils. a) potential respiration, b) moisture content, c) pH, d) total C, e) total S, f) total N.

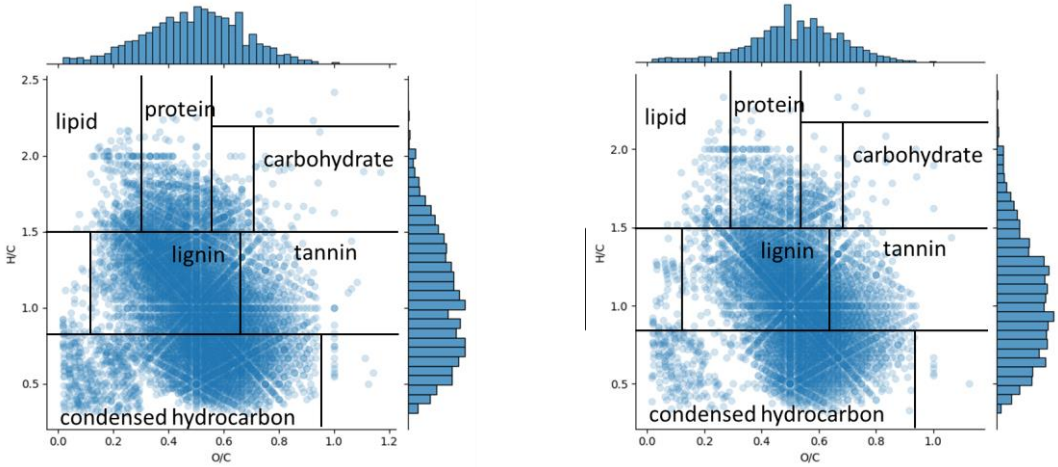

Figure S4 Van Krevelen Diagram of SOM formula identified in a) surface b) subsoils.

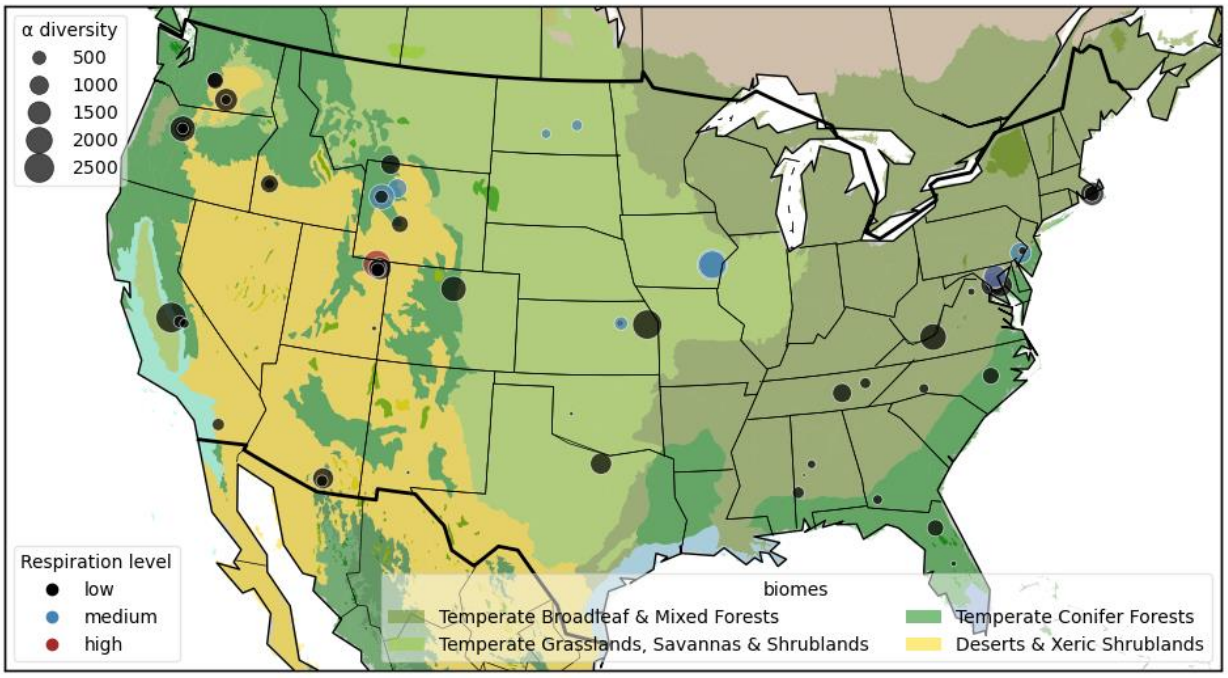

Figure S5. Spatial distribution of subsoil respiration levels (labeled by colors) and alpha diversity of each sample (sizes). Soil respiration levels are determined by K-means clustering on soil respiration rates (ug CO2/g soil/day)

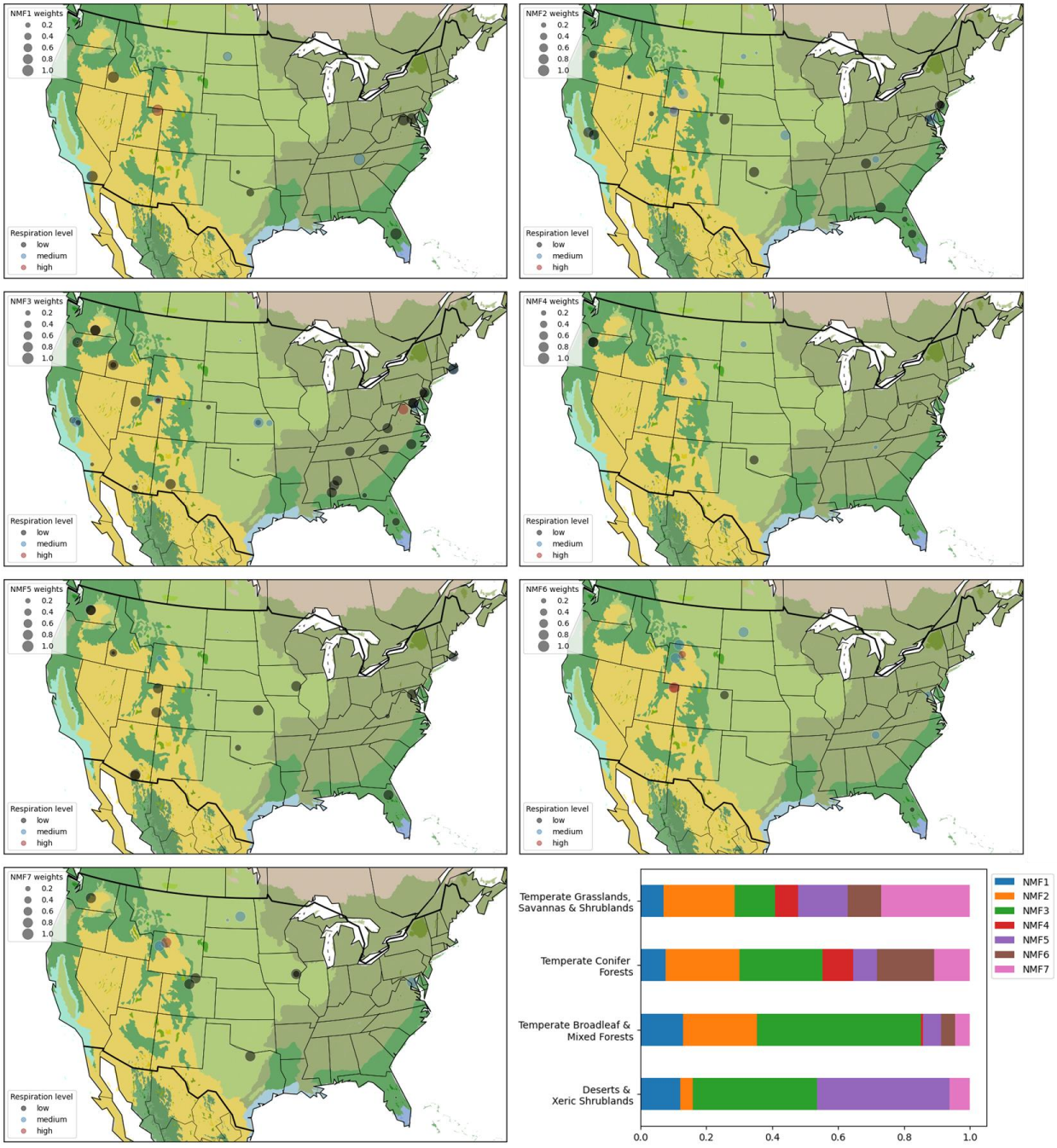

Figure S6. The weights of 7 surface soil SOM types in all samples identified by NMF*k* using SOM composition data obtained from FT-ICR MS, and the relative contribution of the 7 types in each biome. Deserts & Xeric Shrublands (N = 13), Temperate Broadleaf & Mixed Forests (N = 17), Temperate Conifer Forests (N = 21), Temperate Grasslands, Savannas & Shrublands (N = 11).

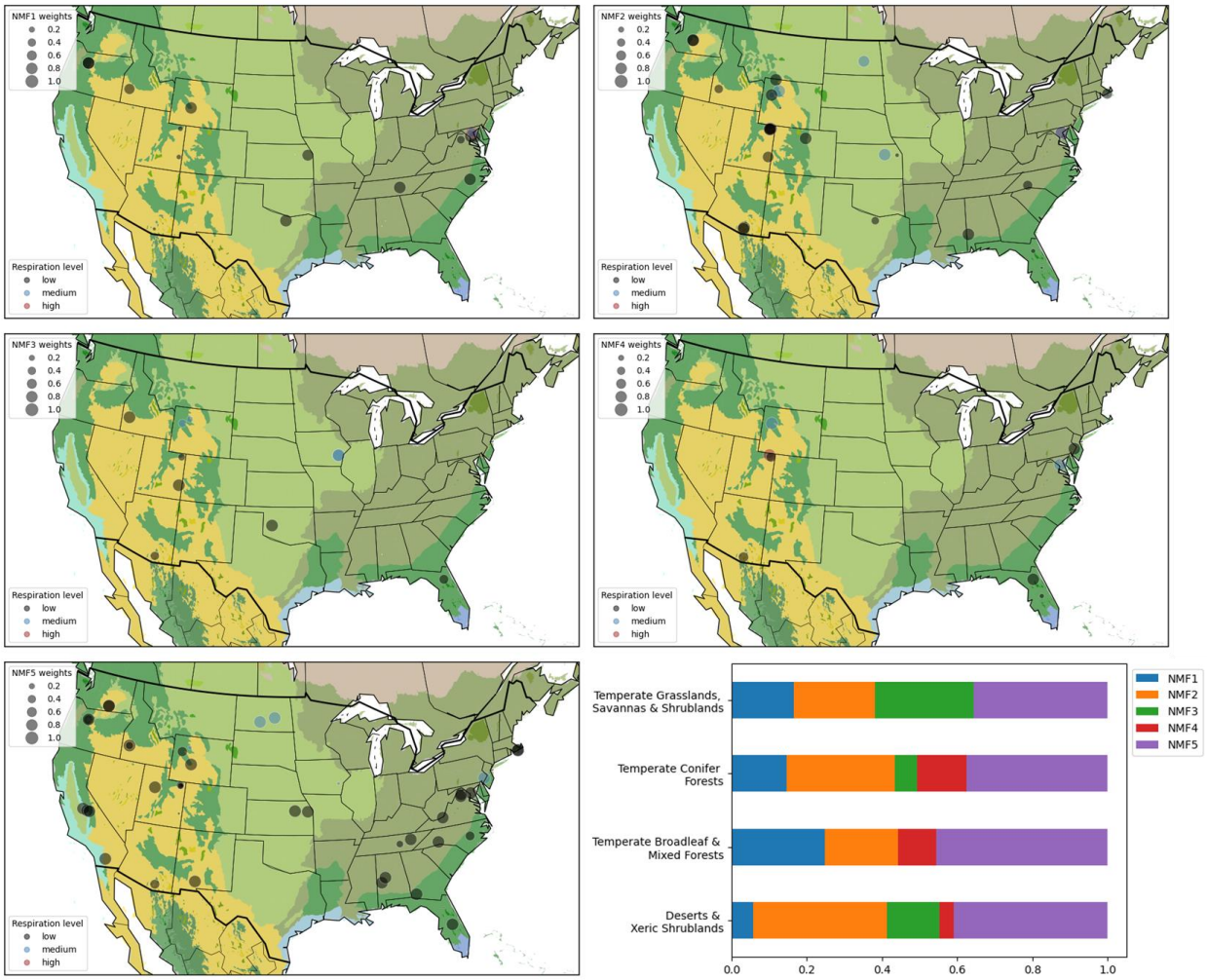

Figure S7. The weights of 5 subsoil SOM types in all samples identified by NMF*k* using SOM composition data obtained from FT-ICR MS, and the relative contribution of the 5 types in each biome. Deserts & Xeric Shrublands (N = 13), Temperate Broadleaf & Mixed Forests (N = 17), Temperate Conifer Forests (N = 21), Temperate Grasslands, Savannas & Shrublands (N = 9).

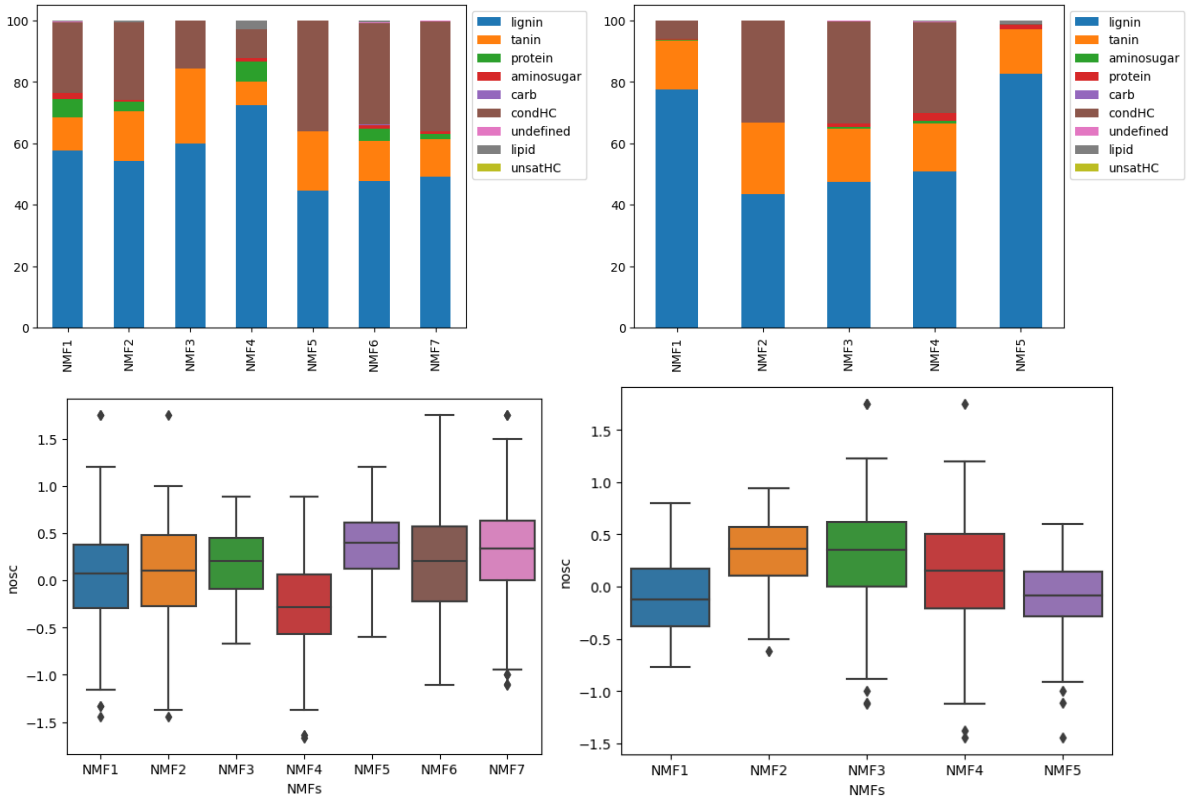

Figure S8. Relative contribution of each compound class to each NMF type for important features with normalized weights of greater than 0.5 in a) surface soil and b) subsoil. Boxplot shows the difference of Nominal Oxidation State of Carbon (NOSC) Values for the important compounds (w > 0.5) for each NMF in c) surface soil and d) subsoil.

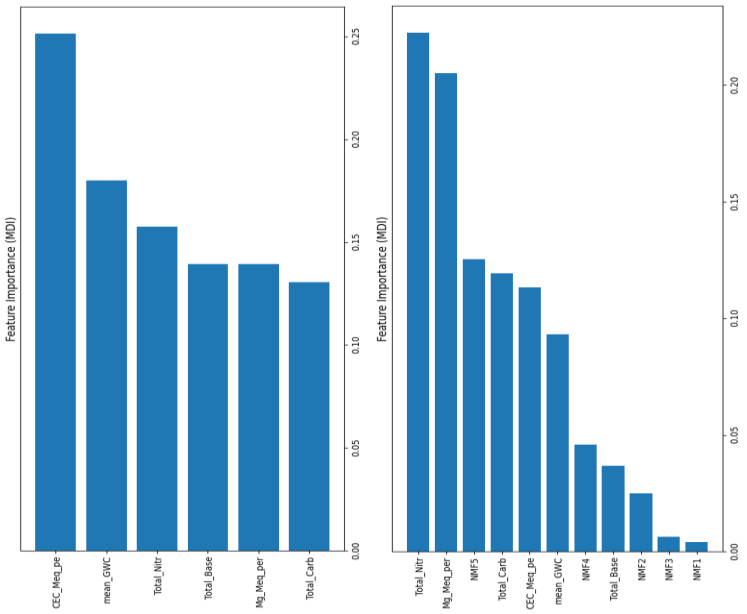

Figure S9. Relative importance of each predictor in subsoil potential respiration models. a) Physicochemical model, with biogeochemical variables only. b) Physicochemistry &SOM_model with both physicochemical variables and SOM types. (SOM model for subsoil has bad performance (Table 1) and therefore feature importance is not reported here).

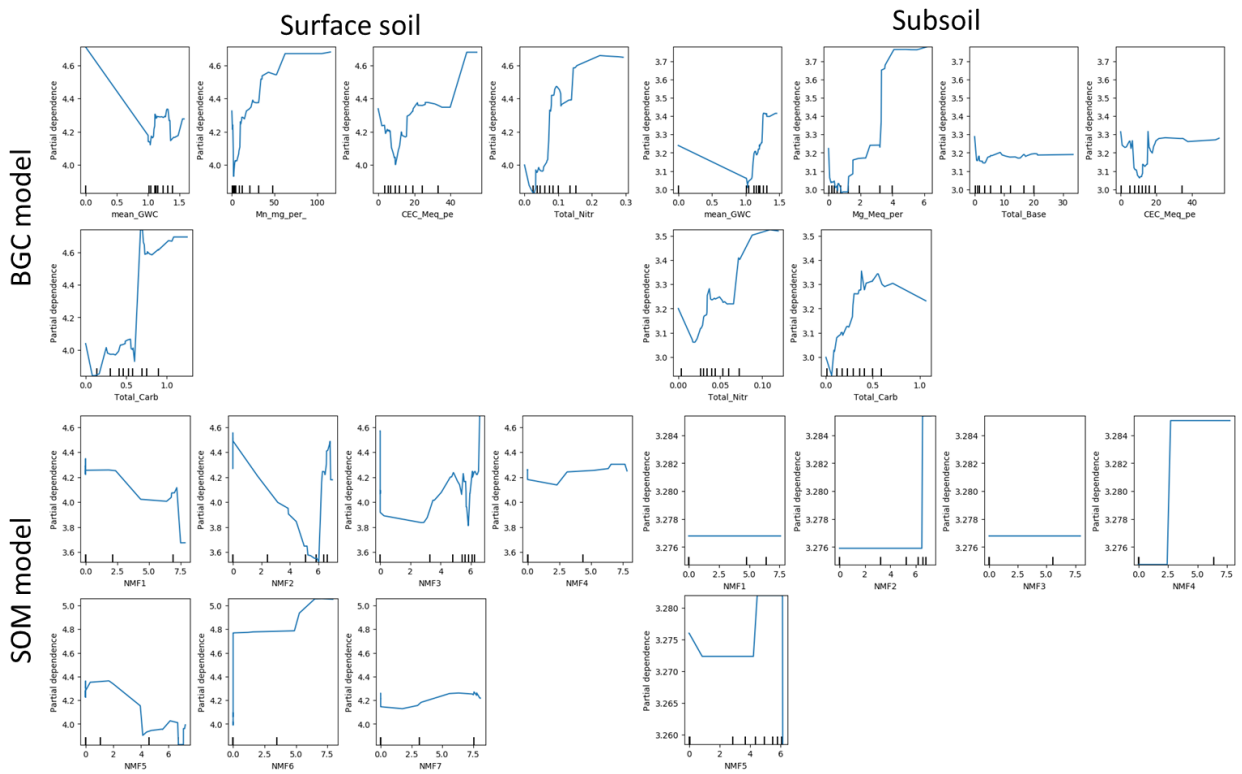
Surface soil
Subsoil
BGC model
SOM model
Partial dependence
mean_GWC
Mn_mg_per_
CEC_Meq_pe
Total_Nitr
Total_Carb
Mg_Meq_per
Total_Base
NMF1
NMF2
NMF3
NMF4
NMF5
NMF6
NMF7

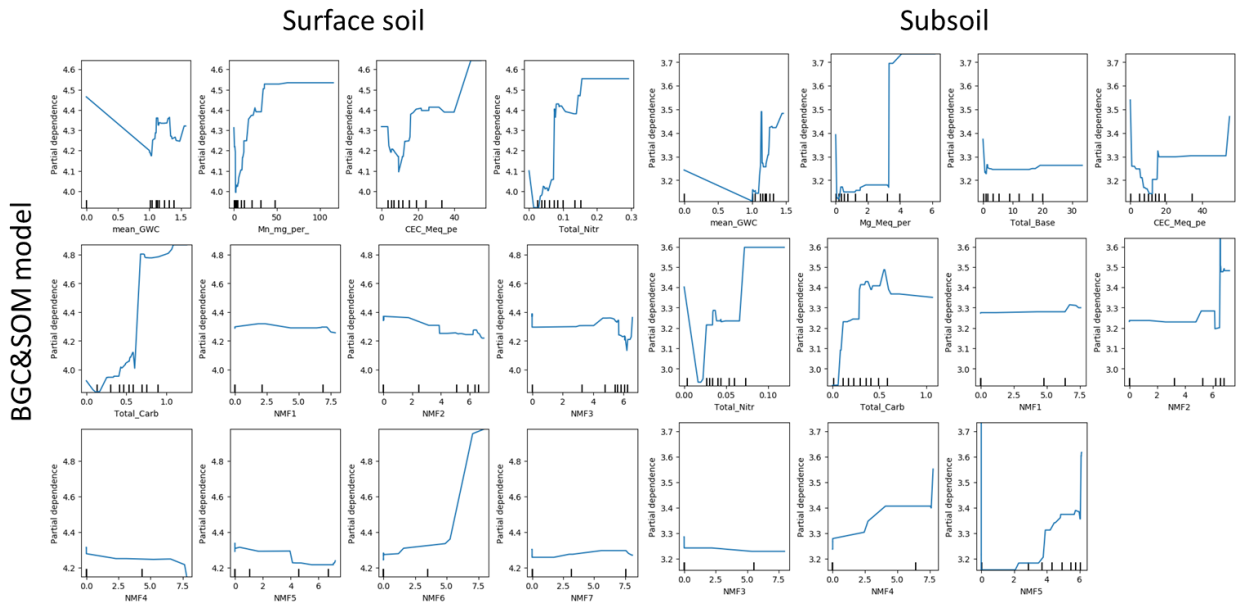
Surface soil
Subsoil
BGC&SOM model
Partial dependence
mean_GWC
Mn_mg_per_
CEC_Meq_pe
Total_Nitr
Mg_Meq_per
Total_Base
Total_Carb
NMF1
NMF2
NMF3
NMF4
NMF5
NMF6
NMF7

Figure S10. Partial dependence of potential respiration to predictors of soil biogeochemistry and/or SOM composition in surface and subsoil models. a) BGC model with biogeochemical variables for surface soil, b) BGC model with biogeochemical variables for subsoi,l c) SOM model with SOM variables for surface soil, d) SOM model with SOM variables for subsoil (bad model performance), e) BGC&SOM model with both biogeochemical and SOM variables for surface soil, f) BGC&SOM model with both biogeochemical and SOM variables for subsoil.

References

1. Brookes, P., et al., *Chloroform fumigation and the release of soil nitrogen: a rapid direct extraction method to measure microbial biomass nitrogen in soil.* Soil biology and biochemistry, 1985. **17**(6): p. 837-842.
2. Witt, C., et al., *A rapid chloroform-fumigation extraction method for measuring soil microbial biomass carbon and nitrogen in flooded rice soils.* Biology and Fertility of Soils, 2000. **30**: p. 510-519.
3. Zhao, Q., et al., *Dynamics of organic matter molecular composition under aerobic decomposition and their response to the nitrogen addition in grassland soils.* Science of the Total Environment, 2022. **806**: p. 150514.
4. Corbridge, D.E.C., *Phosphorus. An outline of its chemistry, biochemistry, and technology*. 1980: Elsevier Scientific Co.
5. Bray, R.H. and L.T. Kurtz, *Determination of total, organic, and available forms of phosphorus in soils.* Soil science, 1945. **59**(1): p. 39-46.
6. AOAC, I., *AOAC Official Method 972.43, Microchemical determination of carbon, hydrogen, and nitrogen, automated method.* Official Methods of Analysis of AOAC International. AOAC International, Gaithersburg, MD, 2006: p. 5-6.
7. Bowman, M.M., et al., *One thousand soils for molecular understanding of belowground carbon cycling.* Frontiers in Soil Science, 2023. **3**.
8. Dittmar, T., et al., *A simple and efficient method for the solid-phase extraction of dissolved organic matter (SPE-DOM) from seawater.* Limnology and Oceanography: Methods, 2008. **6**(6): p. 230-235.
9. Lee, D. and H.S. Seung, *Algorithms for non-negative matrix factorization.* Advances in neural information processing systems, 2000. **13**.
10. Paatero, P. and U. Tapper, *Positive matrix factorization: A non-negative factor model with optimal utilization of error estimates of data values.* Environmetrics, 1994. **5**(2): p. 111-126.
11. Johnson, G.W., et al., *Principal components analysis and receptor models in environmental forensics*, in *Introduction to environmental forensics*. 2015, Elsevier. p. 609-653.
12. Rodenburg, L.A., et al., *Source apportionment of polychlorinated biphenyls in the New York/New Jersey Harbor.* Chemosphere, 2011. **83**(6): p. 792-798.
13. Pauca, V.P., et al. *Text mining using non-negative matrix factorizations*. in *Proceedings of the 2004 SIAM international conference on data mining*. 2004. SIAM.
14. Guillamet, D. and J. Vitria. *Non-negative matrix factorization for face recognition*. in *Catalonian Conference on Artificial Intelligence*. 2002. Springer.
15. Vesselinov, V.V., B.S. Alexandrov, and D. O'Malley, *Contaminant source identification using semi-supervised machine learning.* Journal of Contaminant Hydrology, 2018. **212**: p. 134-142.
16. Cai, Y., H. Gu, and T. Kenney, *Learning Microbial Community Structures with Supervised and Unsupervised Non-negative Matrix Factorization.* Microbiome, 2017. **5**(1): p. 110.
17. Vangara, R., et al., *Finding the Number of Latent Topics With Semantic Non-Negative Matrix Factorization.* IEEE Access, 2021. **9**: p. 117217-117231.
18. Bhattarai, M., et al. *Distributed Non-Negative Tensor Train Decomposition*. in *2020 IEEE High Performance Extreme Computing Conference (HPEC)*. 2020.
19. Friedman, J.H., *Greedy function approximation: a gradient boosting machine.* Annals of statistics, 2001: p. 1189-1232.
20. Hastie, T., et al., *The elements of statistical learning: data mining, inference, and prediction*. Vol. 2. 2009: Springer.
21. Christ, M., et al., *Time Series FeatuRe Extraction on basis of Scalable Hypothesis tests (tsfresh – A Python package).* Neurocomputing, 2018. **307**: p. 72-77.
22. Yuan, B., et al., *Using Machine Learning to Discern Eruption in Noisy Environments: A Case Study Using CO2-Driven Cold-Water Geyser in Chimayó, New Mexico.* Seismological Research Letters, 2019. **90**(2A): p. 591-603.
23. Riaz, M. and P. Marschner, *Sandy Soil Amended with Clay Soil: Effect of Clay Soil Properties on Soil Respiration, Microbial Biomass, and Water Extractable Organic C.* Journal of Soil Science and Plant Nutrition, 2020. **20**(4): p. 2465-2470.

24. Lee, K.-H. and S. Jose, *Soil respiration, fine root production, and microbial biomass in cottonwood and loblolly pine plantations along a nitrogen fertilization gradient.* Forest Ecology and Management, 2003. **185**(3): p. 263-273.
25. Chen, S., et al., *Global annual soil respiration in relation to climate, soil properties and vegetation characteristics: Summary of available data.* Agricultural and Forest Meteorology, 2014. **198-199**: p. 335-346.
26. Waring, B.G., et al., *From pools to flow: The PROMISE framework for new insights on soil carbon cycling in a changing world.* Global Change Biology, 2020. **26**(12): p. 6631-6643.
27. Falloon, P., et al., *Direct soil moisture controls of future global soil carbon changes: An important source of uncertainty.* Global Biogeochemical Cycles, 2011. **25**(3).
28. Orchard, V.A. and F. Cook, *Relationship between soil respiration and soil moisture.* Soil Biology and Biochemistry, 1983. **15**(4): p. 447-453.
29. Xu, L., D.D. Baldocchi, and J. Tang, *How soil moisture, rain pulses, and growth alter the response of ecosystem respiration to temperature.* Global Biogeochemical Cycles, 2004. **18**(4).
30. Moyano, F.E., S. Manzoni, and C. Chenu, *Responses of soil heterotrophic respiration to moisture availability: An exploration of processes and models.* Soil Biology and Biochemistry, 2013. **59**: p. 72-85.
31. Graham, E.B. and K.S. Hofmockel, *Ecological stoichiometry as a foundation for omics-enabled biogeochemical models of soil organic matter decomposition.* Biogeochemistry, 2022. **157**(1): p. 31-50.
32. Wang, Y.-P. and B.Z. Houlton, *Nitrogen constraints on terrestrial carbon uptake: Implications for the global carbon-climate feedback.* Geophysical Research Letters, 2009. **36**(24).
33. Elser, J., et al., *Biological stoichiometry from genes to ecosystems.* Ecology letters, 2000. **3**(6): p. 540-550.
34. Soong, J.L., et al., *Microbial carbon limitation: The need for integrating microorganisms into our understanding of ecosystem carbon cycling.* Global change biology, 2020. **26**(4): p. 1953-1961.
35. Nicolás, C., et al., *The soil organic matter decomposition mechanisms in ectomycorrhizal fungi are tuned for liberating soil organic nitrogen.* The ISME Journal, 2019. **13**(4): p. 977-988.
36. Subedi, P., et al., *The effects of nutrient limitations on microbial respiration and organic matter decomposition in a Florida Spodosol as influenced by historical forest management practices.* Forest Ecology and Management, 2021. **479**: p. 118592.
37. Mori, T., et al., *Reconsidering the phosphorus limitation of soil microbial activity in tropical forests.* Functional Ecology, 2018. **32**(5): p. 1145-1154.
38. Fan, B., et al., *Potential gross nitrogen mineralization and its linkage with microbial respiration along a forest transect in eastern China.* Applied Soil Ecology, 2022. **171**: p. 104347.
39. Gransee, A. and H. Führs, *Magnesium mobility in soils as a challenge for soil and plant analysis, magnesium fertilization and root uptake under adverse growth conditions.* Plant and Soil, 2013. **368**(1): p. 5-21.
40. Opfergelt, S., et al., *The influence of weathering and soil organic matter on Zn isotopes in soils.* Chemical Geology, 2017. **466**: p. 140-148.
41. Chao, L., et al., *Litter carbon and nutrient chemistry control the magnitude of soil priming effect.* Functional Ecology, 2019. **33**(5): p. 876-888.
42. Neupane, A., et al., *Manganese effects on plant residue decomposition and carbon distribution in soil fractions depend on soil nitrogen availability.* Soil Biology and Biochemistry, 2023. **178**: p. 108964.
43. Kranabetter, J.M., T. Philpott, and D. Dunn, *Manganese limitations and the enhanced soil carbon sequestration of temperate rainforests.* Biogeochemistry, 2021. **156**(2): p. 195-209.
44. Santos, F. and E. Herndon, *Plant-Soil Relationships Influence Observed Trends Between Manganese and Carbon Across Biomes.* Global Biogeochemical Cycles, 2023. **37**(1): p. e2022GB007412.
45. Li, H., et al., *A critical review on the multiple roles of manganese in stabilizing and destabilizing soil organic matter.* Environmental science & technology, 2021. **55**(18): p. 12136-12152.
46. Whalen, E.D., *Manganese Limitation as a Mechanism for Reduced Decomposition in Soils under Long-Term Atmospheric Nitrogen Deposition*. 2017, University of New Hampshire.
47. Taylor, P.G. and A.R. Townsend, *Stoichiometric control of organic carbon–nitrate relationships from soils to the sea.* Nature, 2010. **464**(7292): p. 1178-1181.
48. Zhang, M., et al., *The stronger impact of inorganic nitrogen fertilization on soil bacterial community than organic fertilization in short-term condition.* Geoderma, 2021. **382**: p. 114752.
49. Nissan, A., et al., *Global warming accelerates soil heterotrophic respiration.* Nature Communications, 2023. **14**(1): p. 3452.

50. Siles, J.A., et al., *Altitudinal, seasonal and interannual shifts in microbial communities and chemical composition of soil organic matter in Alpine forest soils.* Soil Biology and Biochemistry, 2017. **112**: p. 1-13.
51. Berryman, E.M., J.D. Marshall, and K. Kavanagh, *Decoupling litter respiration from whole-soil respiration along an elevation gradient in a Rocky Mountain mixed-conifer forest.* Canadian Journal of Forest Research, 2014. **44**(5): p. 432-440.
52. Brye, K.R., et al., *Environmental controls on soil respiration across a southern US climate gradient: a meta-analysis.* Geoderma Regional, 2016. **7**(2): p. 110-119.
53. Bond-Lamberty, B. and A. Thomson, *Temperature-associated increases in the global soil respiration record.* Nature, 2010. **464**(7288): p. 579-582.
54. Curiel Yuste, J., et al., *Microbial soil respiration and its dependency on carbon inputs, soil temperature and moisture.* Global Change Biology, 2007. **13**(9): p. 2018-2035.
55. Fang, C. and J.B. Moncrieff, *The variation of soil microbial respiration with depth in relation to soil carbon composition.* Plant and Soil, 2005. **268**: p. 243-253.
56. Kallenbach, C.M., S.D. Frey, and A.S. Grandy, *Direct evidence for microbial-derived soil organic matter formation and its ecophysiological controls.* Nature Communications, 2016. **7**(1): p. 13630.
57. Roth, V.-N., et al., *Persistence of dissolved organic matter explained by molecular changes during its passage through soil.* Nature Geoscience, 2019. **12**(9): p. 755-761.
58. Zhao, Q., et al., *Strong mineralogic control of soil organic matter composition in response to nutrient addition across diverse grassland sites.* Science of The Total Environment, 2020. **736**: p. 137839.
59. Rumpel, C. and I. Kögel-Knabner, *Deep soil organic matter—a key but poorly understood component of terrestrial C cycle.* Plant and soil, 2011. **338**: p. 143-158.
60. Kögel-Knabner, I., *The macromolecular organic composition of plant and microbial residues as inputs to soil organic matter.* Soil Biology and Biochemistry, 2002. **34**(2): p. 139-162.
61. Kramer, C. and G. Gleixner, *Soil organic matter in soil depth profiles: Distinct carbon preferences of microbial groups during carbon transformation.* Soil Biology and Biochemistry, 2008. **40**(2): p. 425-433.
62. Davenport, R., et al., *Decomposition decreases molecular diversity and ecosystem similarity of soil organic matter.* Proceedings of the National Academy of Sciences, 2023. **120**(25): p. e2303335120.
63. Jones, D.L., *Amino acid biodegradation and its potential effects on organic nitrogen capture by plants.* Soil biology and biochemistry, 1999. **31**(4): p. 613-622.
64. Marschner, B. and K. Kalbitz, *Controls of bioavailability and biodegradability of dissolved organic matter in soils.* Geoderma, 2003. **113**(3-4): p. 211-235.
65. Lehmann, J., et al., *Persistence of soil organic carbon caused by functional complexity.* Nature Geoscience, 2020. **13**(8): p. 529-534.
66. Angst, G., et al., *Plant- or microbial-derived? A review on the molecular composition of stabilized soil organic matter.* Soil Biology and Biochemistry, 2021. **156**: p. 108189.
67. Zhang, H., et al., *Microbial dynamics and soil physicochemical properties explain large-scale variations in soil organic carbon.* Global Change Biology, 2020. **26**(4): p. 2668-2685.